EFFECT OF DIFFERENT MOISTURE CONTENT ON THE MIGRATION BEHAVIOUR OF LNAPL IN AGGREGATED KAOLIN USING LIGHT REFLECTION METHOD

SHIRLY CHOW WANNYEN

B.ENG (HONS.) CIVIL ENGINEERING

UNIVERSITI MALAYSIA PAHANG

UNIVERSITI MALAYSIA PAHANG

DECLARATION OF THESIS AND COPYRIGHT

Author's full name : SHIRLY CHOW WANNYEN

Date of birth : 18 MARCH 1992

Title : EFFECT OF DIFFERENT MOISTURE CONTENT ON THE

 MIGRATION BEHAVIOUR OF LNAPL IN AGGREGATED

 KAOLIN USING LIGHT REFLECTION METHOD

Academic Session : 2015/2016

I declare that this thesis is classified as:

☐	**CONFIDENTIAL**	(Contains confidential information under the Official Secret Act 1972)*
☐	**RESTRICTED**	(Contains restricted information as specified by the organization where research was done)*
☑	**OPEN ACCESS**	I agree that my thesis to be published as online open access (Full text)

I acknowledge that Universiti Malaysia Pahang reserve the right as follows:

1. The Thesis is the Property of Universiti Malaysia Pahang
2. The Library of Universiti Malaysia Pahang has the right to make copies for the purpose of research only.
3. The Library has the right to make copies of the thesis for academic exchange.

Certified By:

_____   _____
(Student's Signature)   (Signature of Supervisor)

920318-14-5560   DR. NGIEN SU KONG

New IC / Passport Number   Name of Supervisor
Date :   Date :

NOTES: *If the thesis is CONFIDENTIAL or RESTRICTED, please attach with the letter from the organization with period and reasons for confidentiality or restriction.

EFFECT OF DIFFERENT MOISTURE CONTENT ON THE MIGRATION BEHAVIOUR OF LNAPL IN AGGREGATED KAOLIN USING LIGHT REFLECTION METHOD

SHIRLY CHOW WANNYEN

Thesis submitted in fulfilment of the requirements

for the award of the degree of

B.Eng. (Hons.) Civil Engineering

Faculty of Civil Engineering & Earth Resources

UNIVERSITI MALAYSIA PAHANG

JUNE 2016

SUPERVISORS'S DECLARATION

I hereby declare that I have checked this thesis and in my opinion, this thesis is adequate in terms of scope and quality for the event of the degree of Bachelor of Civil Engineering (Hons.).

Signature:

Name of Supervisor: DR. NGIEN SU KONG

Position: Senior Lecturer

Date:

STUDENT'S DECLARATION

I hereby declare that the work in this thesis is my own except for quotation and summaries which have been duly acknowledged. The thesis has not been accepted for any degree and is not concurrently submitted for award of other degree.

Signature:

Name: SHIRLY CHOW WANNYEN

ID NUMBER: AA12219

Date:

This thesis is dedicated to my beloved family, partner and belated auntie.

ACKNOWLEDGEMENT

I am grabbing this opportunity to express my gratitude to everyone who supported me throughout the course of this final year project. I am thankful for their aspiring guidance and valuable advice during the entire project. I am grateful for their truthful views and kind helps on some issues related to the project.

First and foremost, I would like express my deepest gratitude to my research supervisor, Dr. Ngien Su Kong. The door of his office was always open whenever I had doubt on my research and writing. He consistently steered me in the right direction on the path of research. He always provided me constructive comments with his insight expertise during discussion.

Getting through my research required many laboratory tests, and I would like to express special appreciation to the team of Soil Mechanics and Geotechnical Laboratory, Universiti Malaysia Pahang. I am thankful to the team for their practical guidance and technical advice on operating the equipment in laboratory. Their encouragement and assistance are the factors that drove the laboratory tests towards success.

Furthermore, I would like to express my sincere gratitude to Mdm. Norazimah binti Abdul Aziz from Environmental Engineering Laboratory, Universiti Malaysia Pahang. I am grateful for her useful advice on health and safety prior to the conduct of research. The research was carried out in a safe and sound condition with proper safety instruction from her.

In addition, I would like to express my profound gratitude to my friends, Lim Chia Ni and Ho Xi Cui. I am indebted to them for being supportive throughout the whole research. Their sensible opinions during discussion always enlightened me on solving difficulties I faced in research.

Last but not least, I would like to express my warm thanks to my family and Mr. Teo Kah Wei. I am thankful to them for supporting me spiritually throughout the research and writing of thesis. This accomplishment would not have been possible without their care and support.

I place on record, my sense of gratitude to one and all, who directly and indirectly, have lent their helping hands in this venture.

ABSTRACT

In this research, Light Reflection Method was used to investigate the effect of different moisture content on the migration behaviour of LNAPL in aggregated kaolin. Contamination of groundwater and soil raised the concern on the migration behaviour of LNAPL to aid in remediation research. Therefore, this research was conducted to study the migration behaviour of LNAPL in double porosity media of moisture content 27 %, 29 %, 31 % and 33 %. Photographic method was used to acquire images during the experiments. Image analysis technique was applied to acquire data of research using software Image-Pro Premier 9.1. Based on the findings, LNAPL migrated at the fastest rate with the highest velocity in aggregated kaolin of 31 % moisture content due to larger inter-aggregate pore space when moisture content increased. Other than that, the area of LNAPL migration is the smallest in aggregated kaolin of 31 % moisture content due to higher residual saturation in the larger pore space. The final saturation of 31 % moisture content aggregated kaolin is the lowest due to the weaker capillary pressure in larger pore space. The mean intensity of the LNAPL migration is more uniform in aggregated kaolin of 31 % moisture content because disturbance on light intensity was greatly reduced with the shortest duration of migration. In conclusion, the effect of moisture content on migration behaviour of LNAPL in aggregated kaolin can be investigated using Light Reflection Method. Using photographic method, it has enabled the visualization on LNAPL migration behaviour in aggregated kaolin with data from image analysis.

ABSTRAK

Dalam kajian ini, Kaedah Refleksi Cahaya digunakan untuk mengkaji kesan kandungan lembapan yang berbeza atas migrasi LNAPL dalam kaolin agregat. Pencemaran air bawah tanah dan tanah menimbulkan perhatian pada migrasi LNAPL untuk membantu penyelidikan dalam pemulihan. Oleh itu, kajian ini telah dijalankan untuk mengkaji migrasi LNAPL dalam dual media dengan kandungan lembapan 27%, 29%, 31% dan 33%. Kaedah fotografi telah digunakan untuk memperoleh imej semasa eksperimen. Teknik analisis imej telah digunakan untuk mendapatkan data kajian menggunakan perisian Image-ProPremier 9.1. Berdasarkan dapatan, LNAPL bergerak pada kadar terpantas dengan halaju tertinggi di kaolin agregat yang mengandungi 31% kandungan lembapan kerana ruang liang yang lebih besar apabila kandungan kelembapan meningkat. Selain daripada itu, kawasan migrasi LNAPL di kaolin agregat yang mengandungi kandungan lembapan 31% adalah yang paling kecil disebabkan oleh ketepuan baki yang lebih tinggi di ruang liang yang lebih besar. Ketepuan akhir adalah yang paling rendah untuk kaolin agregat yang mengandungi 31% kandungan lembapan kerana tekanan kapilari yang lebih lemah dalam ruang liang yang lebih besar. Purata keamatan migrasi LNAPL adalah lebih seragam dalam kaolin agregat yang mengandungi kandungan lembapan 31% kerana gangguan pada keamatan cahaya dikurangkan dengan tempoh migrasi yang paling singkat. Kesimpulannya, kesan kelembapan atas migrasi LNAPL dalam kaolin agregat boleh dikaji menggunakan Kaedah Refleksi Cahaya. Dengan menggunakan kaedah fotografi, ia telah membolehkan visualisasi pada migrasi LNAPL dalam kaolin agregat dengan data daripada analisis imej.

TABLE OF CONTENT

CHAPTER 3   METHODOLOGY

CHAPTER 4   RESULTS AND DISCUSSIONS

CHAPTER 5   CONCLUSIONS AND RECOMMENDATIONS

LIST OF TABLES

LIST OF FIGURES

LIST OF SYMBOLS

%	Percentage
γ_w	Wet unit weight of aggregated kaolin
Å	Angstrom
°C	Degree Celsius
C_u	Uniformity coefficient
Cc	Coefficient of gradation
cm	Centimeter
D_{10}	Effective size
d	Penetration
hrs	Hours
LL	Liquid Limit
lm	Lumen
kg	Kilogram
kN	Kilonewton
M	Mass of toluene
m	Meter
mins	Minutes
$m.c$	Moisture content of aggregated kaolin
ρ	Density of toluene
PI	Plasticity Index
PL	Plastic Limit
s	Second
V	Volume of sample

LIST OF ABBREVIATIONS

2D	Two-dimensional
3D	Three-dimensional
ASTM	American Society of the International Association for Testing and Materials
BET	Brunauer-Emmelt-Teller
HSI	Hue, Saturation and Intensity
LNAPL	Light Non-aqueous Phase Liquid
MRI	Magnetic Resonance Imaging
NAPL	Non-aqueous Phase Liquid
NAPLs	Non-aqueous Phase Liquids
ROI	Region of Interest
USCS	Unified Soil Classification System

LIST OF APPENDICES

CHAPTER 1

INTRODUCTION

1.1   BACKGROUND

Non-aqueous Phase Liquids (NAPLs) are hydrocarbons that exist as a separate, immiscible phase when in contact with water and/or air (Newell et al., 1995). NAPLs are classified into Light Non-aqueous Phase Liquid (LNAPL) and Dense Non-aqueous Phase Liquid (DNAPL). LNAPL has density lower than that of water. It passes through unsaturated zone of soil and float on the surface of groundwater. LNAPL is insoluble in water due to the difference in physical and chemical properties between water and NAPL. This causes the LNAPL to form an immiscible liquid phase when it is in contact with water in soil. The migration of LNAPL is also affected by the structure of soil.

The soil categorised as double-porosity media is soil that exhibit two distinct scales of porosity (Sa'ari et al., 2015). Porosity is the amount of voids or air space between the soil particles. The shape and arrangement of soil particles influence the porosity of soil. The presence of inter-aggregate pore and intra-aggregate pore leads to the concept of double porosity. Inter-aggregate pores are pores between soil aggregates. Intra-aggregate pores are pores within the aggregates themselves.

The idea of double-porosity model was initially proposed to describe flow in fractured porous media in the petroleum industry and nowadays, it has developed to the extent of studying the migration behaviour of LNAPL from the geo-environmental aspect. Photographic methods such as the light reflection method are non-destructive and non-intrusive technique used to study the migration of LNAPL. As LNAPL can

pose a great threat to the environment and human health, study on its migration or flow behaviour is essential to aid future research on remediation.

1.2   PROBLEM STATEMENT

Various industrial compounds such as gasoline, diesel fuel, heating oil, solvent, coal tars and chlorinated hydrocarbons are NAPL contaminants. They are typically stored and transported in underground tanks and pipelines which are susceptible to spillage and leakage. Hydrocarbon spilled through the subsurface of soil has caused groundwater pollution. Leakages from underground pipelines, storage tanks and landfills have caused hazardous NAPL contamination in the subsurface of the earth. Due to its highly toxic property, a small amount of NAPL is sufficient to contaminate large area coverage of soil and groundwater. Contaminated groundwater will cause detrimental health problems and is unsafe for drinking purpose. Other than that, contaminated groundwater is unsuitable for industrial and irrigation purpose.

Low flow rate and low solubility together with the uneven distribution of NAPL makes the remediation of NAPL difficult at contaminated sites (Weiner, 2012). Therefore, NAPL is a long-term source of water contamination when they come into contact with soil and groundwater. Hence, it is crucial to understand the migration behaviour of LNAPL to assist in future research on prevention and remediation of LNAPL contamination. However, it is difficult to obtain specific field data to conduct the experiment. Therefore, physical models can be used as a conceptualization mode to study the migration behaviours of LNAPL.

1.3   OBJECTIVES

Clear research objectives are important to guide the research well. The conduct of research must always adhere to the objectives to achieve the expectation. It helps to establish ideas in carrying out the research. The objectives of this research are:

i.   To obtain the properties of the soil used to form the double-porosity samples.

ii.   To investigate the migration behaviour of LNAPL in double porosity soil using photographic method.

iii.   To study the difference in migration behaviour of LNAPL when soil moisture content varies.

1.4   SCOPE OF STUDY

This research was carried out to observe migration behaviour of LNAPL using light reflection method. The physical and chemical properties of soil sample were initially determined before conducting the experiment. The physical properties tests were sieve analysis, hydrometer analysis, liquid limit test, plastic limit test, specific gravity test and falling head test. Since the solid soil sample was used with toxic chemical in this research, Brunauer-Emmett-Teller (BET) and porosity analyzer were used to determine the specific surface area and porosity of soil sample because these two characteristics greatly influence its performance characteristics. All physical properties test were carried out according to ASTM standard. The migration behaviour of toluene was observed in an acrylic model chamber. The dimension of soil sample was 10 cm x 5 cm x 10 cm. This was a qualitative research and the migration behaviour of toluene was observed in soil with 27 %, 29 %, 31 % and 33 % moisture contents respectively. Pouring method was used to transfer chemical to soil sample as a simulation to spillage of LNAPL. The results obtained were analysed using image analysis technique. Image-Pro Premier 9.1 was used to analyse the outcome of experiment.

1.5   SIGNIFICANCE OF STUDY

This research will be a significant endeavour in providing information and data for future research on remediation of LNAPL contamination. LNAPL contamination is a widespread and serious environmental issue, thus, study on the migration behaviour is a prior effort to formulate remediation strategy in addressing the problem. Due to the heterogeneity of subsurface, contaminant behaviour in soils can be very complex. Therefore, laboratory physical model can improve basic understanding of NAPL migration behaviour in the subsurface. The method used in conducting this research,

which is light reflection method, is able to show a clear image for the observation of LNAPL's migration behaviour. Furthermore, this research solve the problem of dealing with very toxic chemicals in field experiments as it is carried out in a physical model at lab which still uses toxic chemical but in a more controlled condition. A better understanding on migration behaviour of LNAPL helps in the establishment of effective remedial measures in dealing with soil and groundwater contamination. Groundwater free of contamination ensures safe and clean water supply.

CHAPTER 2

LITERATURE REVIEW

2.1   LIGHT NON-AQUEOUS PHASE LIQUID (LNAPL)

LNAPLs are those liquid hydrocarbon compounds or mixtures that are less dense than water, such as gasoline and diesel fuels (Weiner, 2012). LNAPL is lighter than water due to smaller density compared to water. Thus, LNAPL is buoyant and it floats on water table in vadose zone. LNAPL moves vertically downward through vadose zone due to gravity force and spread horizontally above groundwater when it encounters the water table. LNAPL exists in different phases such as adsorbed phase, dissolved phase, gaseous phase and free NAPL phase in unsaturated zone. Table 2.1 lists the typical LNAPLs and their properties.

2.2   SOIL SUBSURFACE

The soil subsurface is commonly divided into unsaturated zone and saturated zone based on their air and water content. The unsaturated zone occurs in the upper, near-surface layers of soil that are not fully saturated with water, while the saturated zone typically represents deeper soils wherein all the void spaces between the soil particles are filled up with water (Ramaswami et al., 2005). The water table acts as a divider between the saturated and unsaturated zone. Each zone contains soil particles with pores between the particles. The voids allow movement of water and contaminant plume through them. The soil subsurface with indicated porosity, moisture content and air content is depicted in Figure 2.1.

Table 2.1: Typical LNAPLs and their properties

Chemical	Density (g/cm^3)	Dynamic Viscosity (cP)	Water Solubility (mg/L)	Vapour Pressure (mmHg)	Henry's Law Constant (atm.m^3/mol)
Benzene	0.8765	0.6468	1780	76	5.43 x 10^{-3}
Ethyl benzene	0.867	0.678	152	7	7.9 x 10^{-3}
Toluene	0.8669	0.58	515	22	6.61 x 10^{-3}
o-Xylene	0.880	0.802	170	7	4.94 x 10^{-3}
Methyl ethyl ketone	0.805	0.40	26800	71.2	2.74 x 10^{-3}

Adapted from: Sharma & Reddy (2004)

2.2.1 Unsaturated Zone

The unsaturated zone is also known as the vadose zone. Soil porosity can be used to describe the pore spaces in soil subsurface. The total amount of moisture and air present in the pore spaces represents the soil porosity. Changes in moisture content, Θ_w, affect many physical properties within the vadose zone (Ramaswami et al., 2005). The moisture content increases with the depth of soil until the level of water table where the pore spaces are occupied with water and contain no more air. At this stage, the moisture content is equal to the porosity of soil as depicted in Figure 2.1. The fluid pressure above the water table, i.e., in the vadose zone, is less than atmospheric pressure due to the suction created by the capillary action of the intraparticle void spaces (Ramaswami et al., 2005). The lower the moisture content of soil, the more water will be absorbed and hence, greater suction pressure is produced. According to a research conducted by Sa'ari et al. (2015), the rate of migration of LNAPL was increased when the moisture content increased.
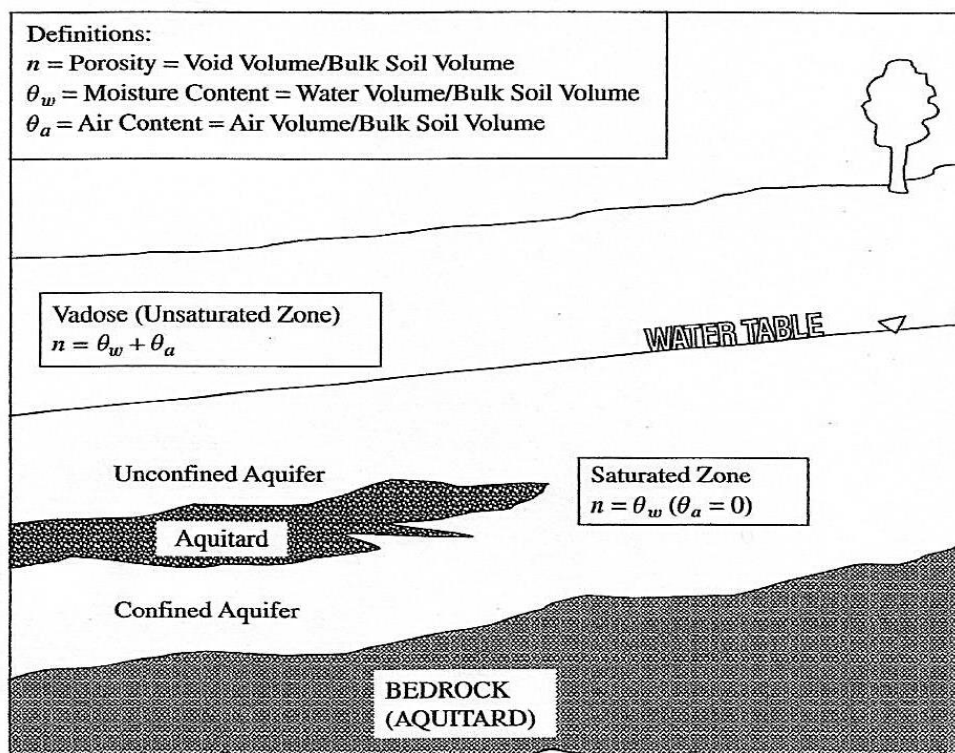
Figure 2.1: Saturated and unsaturated soil zones in the subsurface

Source: Ramaswami et al. (2005)

2.3   SOURCES OF CONTAMINANT IN UNSATURATED ZONE

Various substances deposited in the vadose zone lead to subsurface contamination. Some conditions such as landfills, leakage from underground pipelines, leakage from underground storage tanks, surface impoundments and waste disposal in excavations are typical sources of contamination in the vadose zone. Landfill is a source of contamination because leachates infiltrate into the subsurface and pollute the soil and groundwater. Leakage of buried pipelines that are used to transport liquids is generally difficult to detect and can cause severe contamination. Leakage from underground storage tanks, for instance, gasoline leakage due to corrosion of tank is a major contamination source of soil and groundwater. The risk of subsurface contamination caused by surface impoundment is high because it is usually located in permeable soil in which the wastes can easily infiltrate into the soil. Waste disposal in excavations can

cause extensive contamination due to infiltration of liquid wastes among the unregulated dumps.

2.4 PROPERTIES INFLUENCING MIGRATION OF NAPLs

The most important characteristics that affect the behaviour of NAPLs in the subsurface are density, viscosity, solubility, volatility, interfacial tension, wettability and capillary pressure (Sharma & Reddy, 2004).

2.4.1 Density

Density is the mass of a substance per unit volume (Mercer & Cohen, 1990). The density of water is 1 g/cm^3. LNAPL is lighter than water and float on groundwater because it has density less than 1 g/cm^3. The densities of NAPLs increase with decreasing temperature. As temperature decreases, the molecules of NAPLs are more closely packed together. Therefore, the volumes of NAPLs become smaller due to the inverse relationship between density and temperature. The hydraulic conductivity of NAPLs increase as the density increases.

2.4.2 Viscosity

Viscosity is the internal friction that resists the movement of a liquid (Mercer & Cohen, 1990). The viscosities of NAPLs decrease with increasing temperature. As temperature increases, the molecules of NAPLs gain more energy and become less viscous. Less viscous NAPLs flow more easily in porous medium. It has been proven in the experimental investigation conducted by Borzooei et al. (2014) that the rate of flow in vertical movement of more viscous fluid is slower than less viscous fluid and result in more lateral spread.

2.4.3 Solubility

The aqueous solubility is defined as the maximum concentration of chemical that will dissolve in pure water at a certain temperature (Mercer & Cohen, 1990).

Solubility is used to measure the partitioning of free NAPL phase into dissolved phase, called dissolution. Dissolution rate increase when fraction of soluble components increases. NAPLs are non-polar and low-polarity liquid that are minimally soluble in water (Weiner, 2012). They are made up of molecules that are weakly polar or non-polar. Solubility of NAPLs are low when mixed with water which is made up of highly polar molecules. NAPLs remain as separate, immiscible liquid layers when in contact with water due to weak attraction to polar water molecules.

2.4.4   Volatility

Volatility is used to evaluate the volatilization of NAPLs from the water. Applying Henry's law in the case of single organic compound, the tendency of the organic molecules to escape from liquid to gaseous phase is proportional to the concentration of dissolved organic. Raoult's law is applied on the case of multiple organic compounds where the product of the mole fraction of the solute and the vapour pressure of the pure phase liquid is the vapour pressure over a solution.

2.4.5   Interfacial Tension

Interfacial tension is the surface energy at the interface that results from differences in the attraction force between molecules of two immiscible fluids (Sharma & Reddy, 2004). Low interfacial tension between NAPLs and water enables the NAPL to exist mostly in voids of soil. The lower the interfacial tensions between the NAPLs and water, the weaker the stability of the interface between the liquids. Hence, the migration rate is greater when the interfacial tension is lower.

2.4.6   Wettability

Wettability is the tendency of one fluid to spread on or adhere to a solid surface in the presence of another fluid with which it is immiscible (Mercer & Cohen, 1990). It is used to explain the NAPLs distribution at the pore spaces. According to the concept of wettability, water is a wetting fluid displacing NAPL from pore spaces while air is a non-wetting fluid that allows NAPLs to adhere to soil surfaces. Referring to Figure 2.2,

it is most often quantified with contact angle measurement (Katsifarakis, 2000). The contact angle of wetting liquid is less than 90° whereas the contact angle of non-wetting liquid is more than 90°.
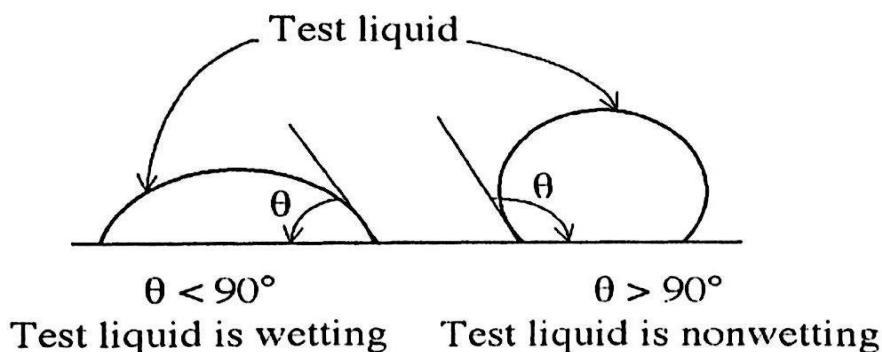
Figure 2.2: Example of contact angle

Source: Katsifarakis (2000)

2.4.7 Capillary Pressure

Capillary pressure is the pressure exerted across the interface between the wetting and non-wetting phases (Mercer & Cohen, 1990). Capillary pressure is a measure of cohesion of liquid molecules and adhesion of liquid molecules which is represented by the tendency of the porous medium to adhere to the wetting fluid and repel the non-wetting fluid (Sharma & Reddy, 2004). Capillary pressure is used to displace wetting liquid originally filling a pore with a non-wetting fluid. The non-wetting liquid is forced into the larger pores due to the resistance of smaller pores towards capillarity.

2.4.8 Soil Structure

Ladd et al. (1996) defined soil structure as the size, shape and arrangement of particles in soils. The migration of contaminant depends on the structure of soil (Sa'ari et al., 2015). The structure of soil influences the hydraulic conductivity of NAPLs.

Hydraulic conductivity refers to the ease with which water can flow through a soil (Sharma & Reddy, 2004). NAPLs flow through a porous media more easily than a less porous media.

2.5   LABORATORY AND NUMERICAL SIMULATIONS OF LNAPL

Laboratory and numerical simulations have been used to study the migration behaviour of LNAPL because field study is infeasible due to the highly toxic characteristic of chemical compounds. The summary of NAPL experiments approach is highlighted in Figure 2.3. Qualitative and quantitative infiltration and redistribution experiments are methods that can be used to study the migration behaviour of LNAPL. Quantitative infiltration and redistribution experiment for LNAPL can be further divided into without numerical modelling and with numerical modelling. Light Reflection Method, Light Transmission Method and Multispectral Image Analysis Method are photographic methods that can be used as saturation imaging technique for NAPLs.

2.6   PREVIOUS STUDIES

The application of laboratory conceptual models has been recognised as a useful tool in geo-environmental investigations. The most distinct advantage of laboratory modelling is time saving and cost effective compared to field investigations which are usually more costly due to the less controllable environment. Imaging methods are often applied in the laboratory investigation of LNAPL's migration behaviour. From the review of Werth et al. (2010), the more widely used imaging techniques are optical imaging using UV or visible light, dual-energy gamma radiation, X-ray microtomography and magnetic resonance imaging (MRI). Optical method is the simplest and most economical approach for imaging pollutant flow and distribution. Gamma radiation is used to perform two-dimensional (2D) characterization of fluid distribution at the Darcy scale. X-ray method provides the highest resolution for three-dimensional (3D) characterization of fluid distribution in natural porous media while MRI is an ideal option for 3D characterization of fluid distribution in artificial porous media. The digital image processing technique using Matlab routine and Surfer software

was applied to show the LNAPL migration behaviour in the soil column physical model conducted by Sa'ari et al. (2015). From the experiment conducted by Sa'ari et al. (2015), the moisture content of kaolin used is limited to 35% because it failed to produce the aggregated kaolin and was difficult to compact during the compaction works if the moisture content exceeds 35%. A proper understanding on the migration behaviour of LNAPL is essential for the design of effective remedial systems. Various remediation processes are adopted in extracting LNAPL from contaminated soil. Several methods such as surfactant flushing, alcohol flushing, soil vapour extraction and air sparging are discussed in the review of Kamaruddin et al. (2011). However, continuous effort on investigation of migration behaviour of LNAPL is needed to figure out more alternatives as remedial of LNAPL. Therefore, toluene migration behaviour is monitored in this research to obtain a better fundamental understanding on migration behaviour of LNAPL in double-porosity media.

Figure 2.3: Methods of NAPL experiments

Source: Oostrom et al. (2006)

CHAPTER 3

METHODOLOGY

3.1   PHYSICAL PROPERTIES TESTS

Sieve analysis, hydrometer analysis, liquid limit test, plastic limit test, specific gravity test and falling head test were used to determine the physical properties of soil. ASTM D 422-63 was used to determine the distribution of particle sizes in soils quantitatively. The distribution of particle sizes larger than 75 μm was determined by sieve analysis while the distribution of particle sizes smaller than 75μm was determined by hydrometer analysis. The soil sample was classified using Unified Soil Classification System (USCS) referring to ASTM D 2487. ASTM D 4318-00 was used to determine the liquid limit and plastic limit of soil sample. Specific gravity of soil sample was determined by means of water pycnometer according to ASTM D 854-02. Laboratory measurement of hydraulic conductivity (also referred to as coefficient of permeability) of soil sample was determined using ASTM D 5084-03. The specific surface area of sample was determined according to the procedure in ASTM D4567-03 while the porosity of sample was determined using ASTM D4641-12.

3.2   LABORATORY EXPERIMENT

Prior to the experiments, some physical properties tests were carried out to determine the properties of the soil sample. Four laboratory experiments were conducted to investigate the effect of different moisture content on the migration behaviour of aggregated kaolin using Light Reflection Method. Each of the laboratory experiment used aggregated kaolin of different moisture content with other parameters

remain constant. The outcome of experiments was analysed using Image-Pro Premier 9.1. Figure 3.1 shows the flow chart of overall procedure in research.

Physical Properties Tests
- Fall Cone Penetration Test
- Hand-rolled method
- Water Pycnometer Test
- Sieve analysis
- Hydrometer analysis
- Falling Head Test
- Single Point BET
- Porosity Analyzer

Laboratory Experiments
- 27 %, 29 %, 31 % and 33 % moisture contents
- Aggregated Kaolin Preparation
- Flow Chamber Preparation
- LNAPL Preparation
- Setup of Camera

Image Analysis
- Image-Pro Premier 9.1
- Microsoft Excel

Figure 3.1: Flow chart of overall procedure in research

3.2.1 Aggregated Kaolin Preparation

S300 kaolin was selected as the soil sample in conducting the experiment. Kaolin was dried in oven at 105 °C for at least 24 hrs before it was mixed with water. Water was added to dried kaolin to prepare aggregated kaolin. Four different water contents of aggregated kaolin were prepared, which are 27 %, 29 %, 31 % and 33 % respectively. The prepared samples were sealed in different plastic bags and pressed carefully to expel trapped air to avoid moisture loss. The samples were kept in a cool and dark place for at least 24 hours to maintain the moisture content. It was essential to make sure the aggregated kaolin was compacted in one lump when it was kept in sealed plastic bag to ensure the moisture content achieve equilibrium state. The aggregated kaolin was then sieved to size 2.00 mm using sieve No.8.

3.2.2 Flow Chamber Preparation

For the purpose of laboratory setup in this qualitative experiment, acrylic chamber that was 30 cm high, 10 cm long and 5 cm wide was chosen as the model for the double-porosity media. The rectangular acrylic chamber provided a clear visualization for observation on migration of LNAPL. The height of flow chamber must be higher than the height of sample to ensure sufficient space for compression of aggregated kaolin that was filled in the chamber. The flow chamber was filled with calculated mass of aggregated kaolin and compressed to required height with an acrylic compression tool to form a sample with 10 cm height, 10 cm length and 5 cm width. Hence, the volume of the sample was 0.0005 m^3. The mass of aggregated kaolin to form the sample was determined using the principle of relationship between density, mass and volume.

The bulk unit weight of kaolin was 11 kN. Since the samples were made up of different moisture contents, the wet unit weight of each sample was identified using Eq. (3.1) as the initial step to find out the mass of aggregated kaolin required to form four 0.0005 m^3 samples.

$$\gamma_w = 11 \times (1 + m.c) \tag{3.1}$$

The unit weight was then multiplied with the volume of sample to obtain the weight of sample in *kN* using Eq. (3.2) as shown below

$$Weight\ of\ sample = \gamma_w \times V \tag{3.2}$$

The weight of sample was converted to *kg* using Eq. (3.3) as the final step to obtain the mass of aggregated kaolin needed to form 0.0005 m^3 sample.

$$Mass\ (kg) = Weight\ (kN) \times \frac{1000\ kg}{9.81\ kN} \tag{3.3}$$

3.2.3 LNAPL Preparation

Toluene was used as a source of LNAPL. It is a clear, flammable and volatile liquid with benzene-like odour as indicated in Material Safety Data Sheet (MSDS) in Appendix A. It is slightly soluble in water and soluble in petroleum ether, alcohol, chloroform, ether, acetone, carbon disulphide, acetate and benzene. Since toluene is colourless, it was dyed red with Oil Red-O for the purpose of visual observation during experiment. During mixing, make sure all the Oil-Red-O was dissolved in toluene so that no residue remained in beaker after pouring of toluene into flow chamber. The red colour also provided distinct recognition in selecting region of interest during analysis using Image-Pro Premier 9.1. The mass of Oil Red-O used was 0.01 % of the mass of toluene. However, the first experiment trial showed that 0.01% of Oil Red-O was insufficient to achieve the expected photo quality because the colour of dyed toluene was too light. Therefore, the amount of Oil Red-O was double up to 0.02 % of the mass of toluene. 43.25 g toluene was poured onto the top surface of sample in flow chamber. The mass of toluene required was calculated using Eq. (3.4).

$$V = 10 \ cm \ \times 5 \ cm \times 1 \ cm$$
$$= 0.00005 \ m^3$$

$$M = \rho \times V \tag{3.4}$$

3.2.4 Digital Camera Setup

Canon EOS Kiss X6i camera with a sensor size of 22.3×14.9 mm and approximately 18.0 megapixels was used to observe the migration behaviour of LNAPL in model chamber. This camera was chosen because it tracks moving objects accurately across the frame and its continuous shooting up to 30 fps enables the quick capturing of image throughout the entire experiment. The camera was mounted on a tripod which was located at a distance of 1 m away from the flow chamber. Canon EOS Utility was used to remote image capturing during experiment to avoid displacement of camera position. The camera setting was adjusted to exposure time of 1/30, ISO speed of ISO-800 and focal length of f/5.6 to capture clear images during the experiments. Each

image was taken at every 5 seconds interval. The camera captured the image once the toluene was poured into flow chamber.

3.3   IMAGE ANALYSIS TECHNIQUE

Light reflection method was associated with image analysis technique to produce highly reliable saturation image for analysing LNAPL migration in 2-D chamber model. The images captured during experiment were converted to hue, saturation and intensity (HSI) format for data interpretation. The images were analysed according to the general steps in flow chart shown in Figure 3.2.

Image measurement was calibrated into actual size.

A region of interest was selected.

Object and background were distinguished using smart segmentation.

Analysis was run and types of measurement were selected.

Data were exported to Microsoft Excel.
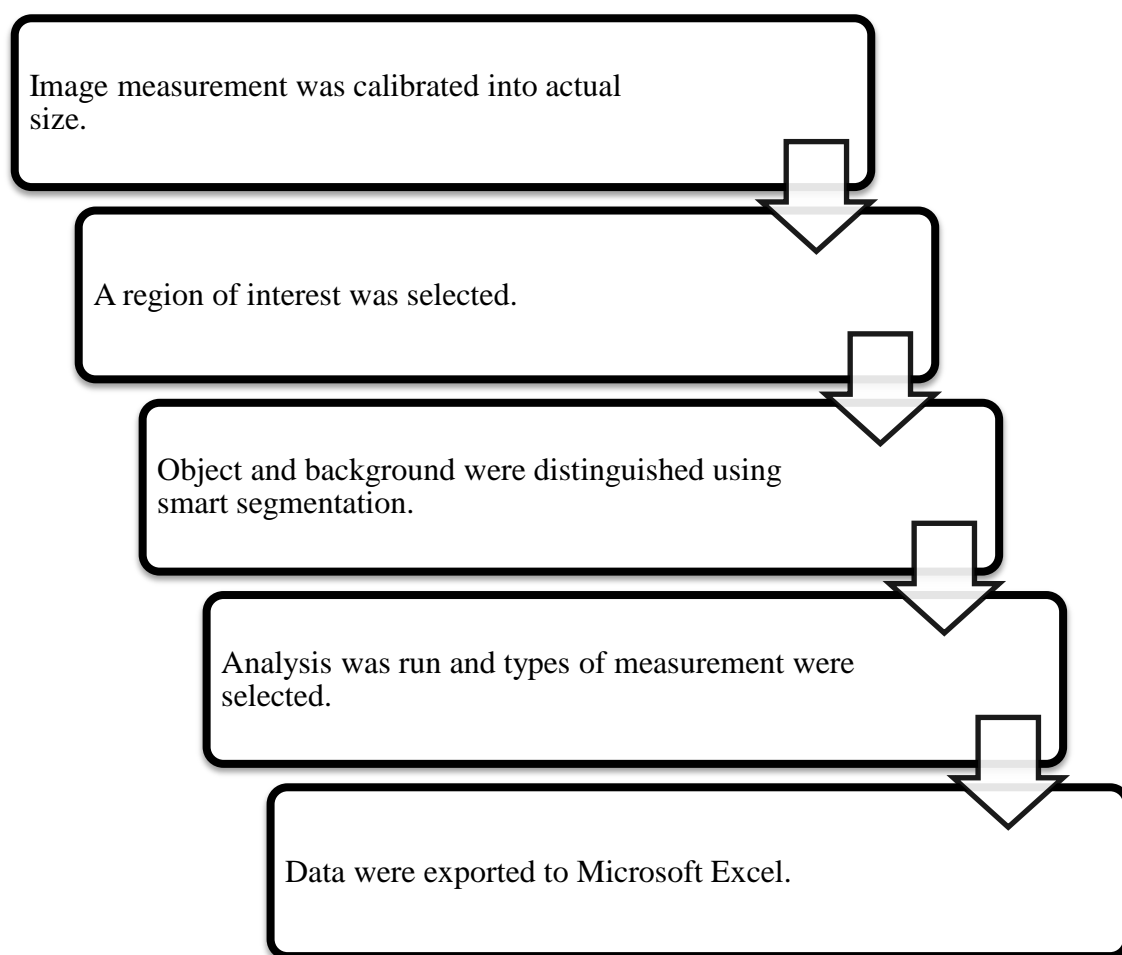
Figure 3.2: Steps in image analysis using Image-Pro Premier 9.1

Calibration was vitally important because it defines the accuracy of measurement in analysis. A proper calibration on measurement of object into actual size was the prior step in analysis using Image-Pro Premier 9.1. First of all, the *Spatial Calibration* button in *Calibration* group under the *Capture* ribbon was clicked. A dialog of *Spatial Calibration* appeared on the right hand side of interface as shown in Figure 3.3.
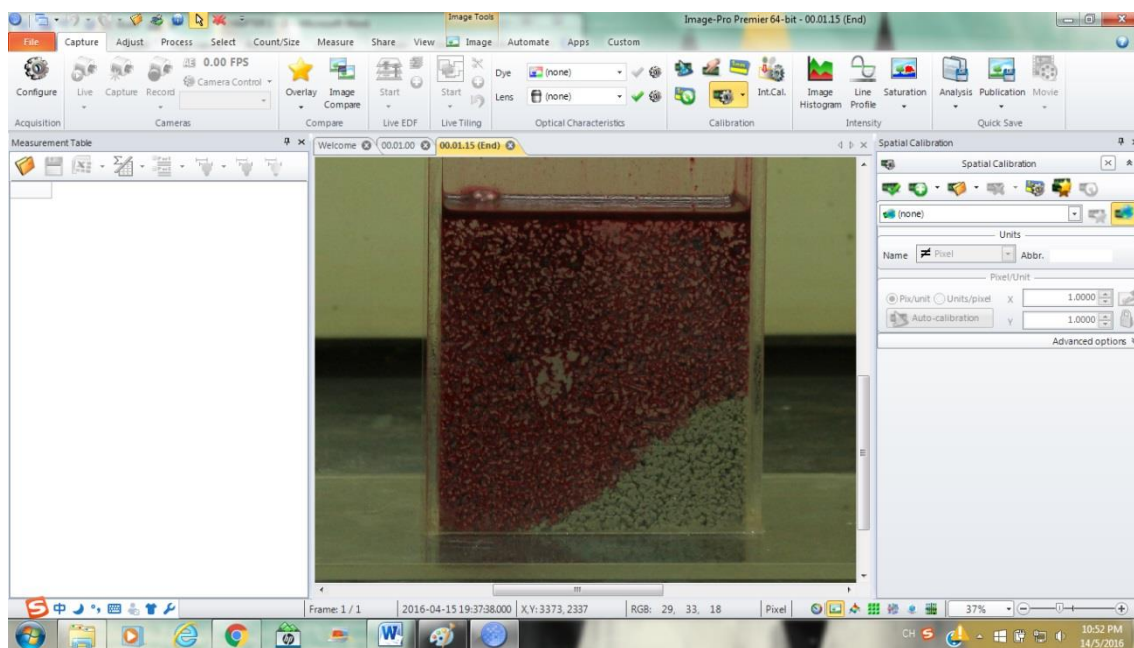
Figure 3.3: Spatial calibration dialog

To calibrate the object measurement into actual size, *Quick Calibration* button in *Calibration* group under the *Capture* ribbon was chosen and a reference line was drawn as shown in Figure 3.4. Then, the reference length and unit were input in the popup dialog and Ok button was clicked. A new spatial calibration was created and applied to the active image using the *Apply* button in *Spatial Calibration* dialog as shown in Figure 3.5.

Since only the sample coverage was the region to be analysed, it was essential to select *Region of Intereest (ROI)* using a rectangle tool in *Region of Interest* group under the *Select* ribbon as shown in Figure 3.6. This was to clearly separate the region to be analysed from the unrelated region in image to obtain an accurate result.
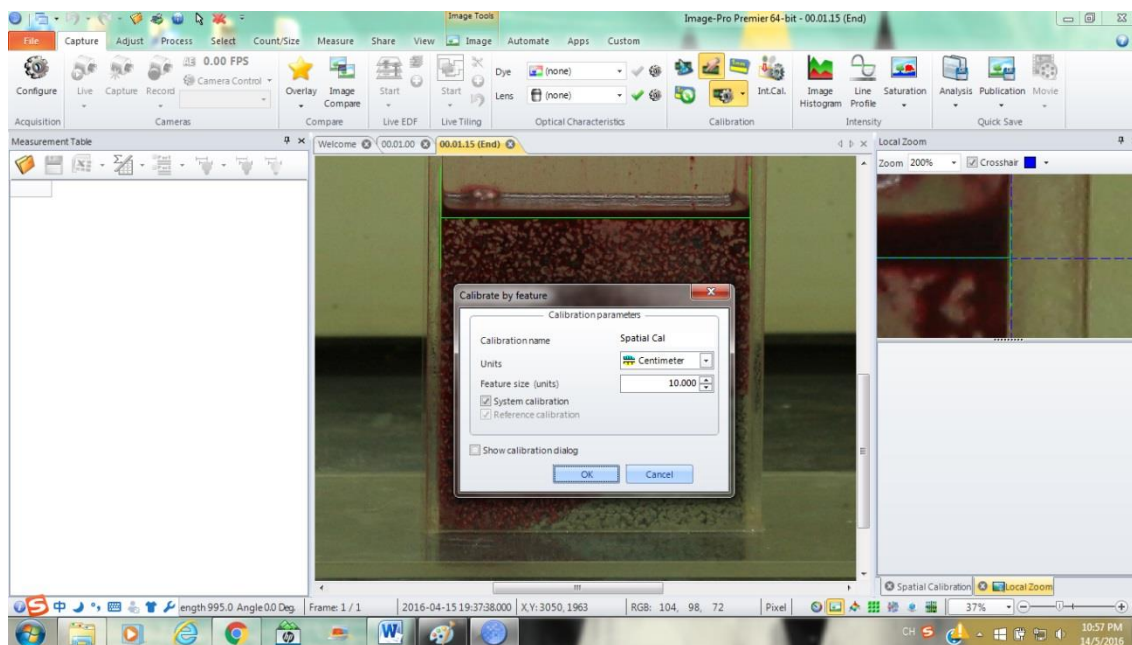
Figure 3.4: Drawing reference line to create spatial calibration
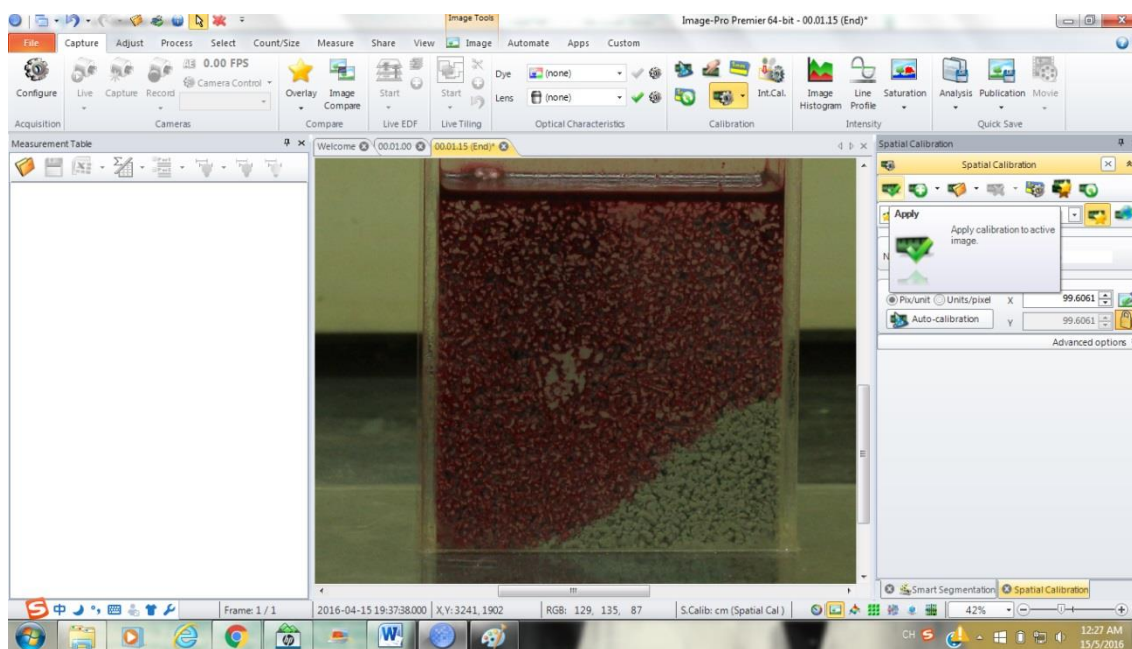
Figure 3.5: Applying spatial calibration
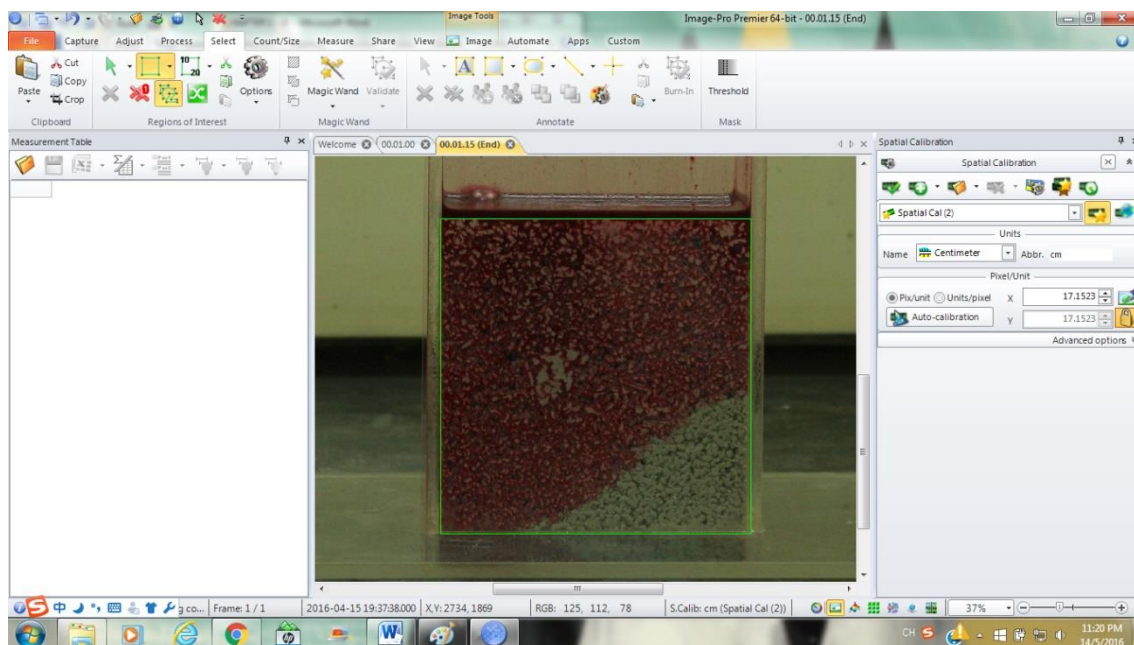
Figure 3.6: Selecting *Region of Interest*

In the region of interest, the area of soil sample contaminated with LNAPL was defined as object while the area of uncontaminated soil sample was defined as background. The object and background were markedly defined using *Smart Segmentation* function in *Segment* group under the *Count/Size* ribbon as shown in Figure 3.7. A blue ellipse was drawn on the object area while a yellow ellipse was drawn on the background area.

There were various types of measurement that can be obtained from analysis using Image-Pro Premier 9.1. Hence, it was better to select only the types of measurement needed to be displayed before running an analysis. This was done by adding the desired measurements in *Type* option in *Measurement* group under the *Count/Size* ribbon as shown in Figure 3.8.

After selecting the types of measurement, the *Count* button in *Smart Segmentation* dialog was clicked to generate analysis as shown in Figure 3.9. The desired measurements obtained from analysis were displayed in a *Measurement Table*.
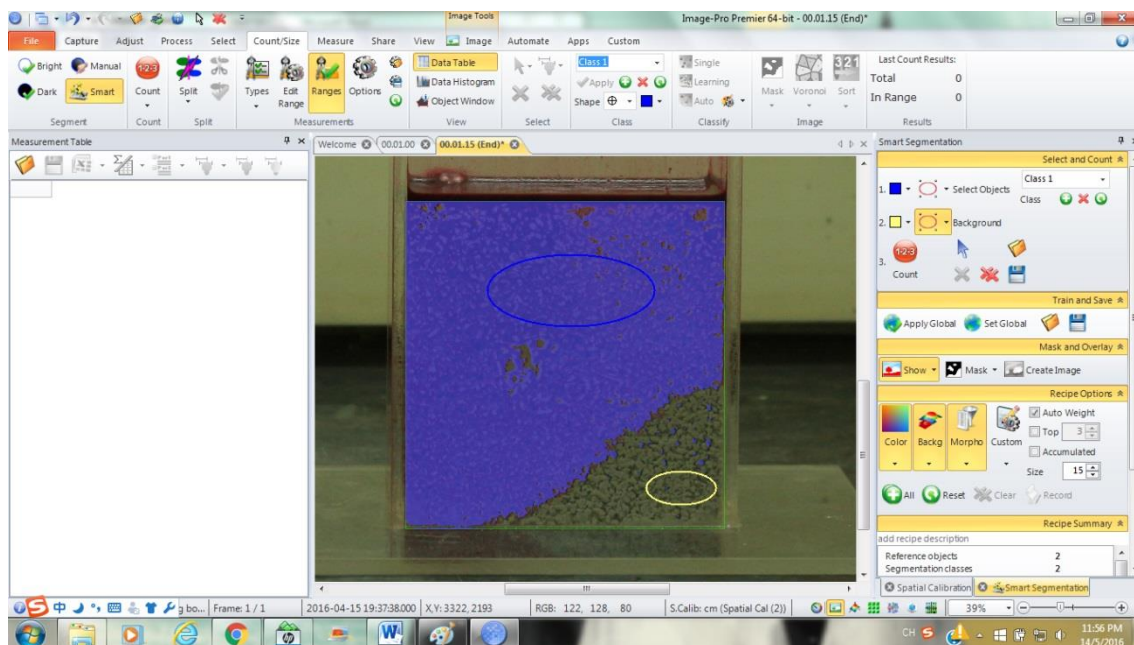
Figure 3.7: Smart segmentation of object and background
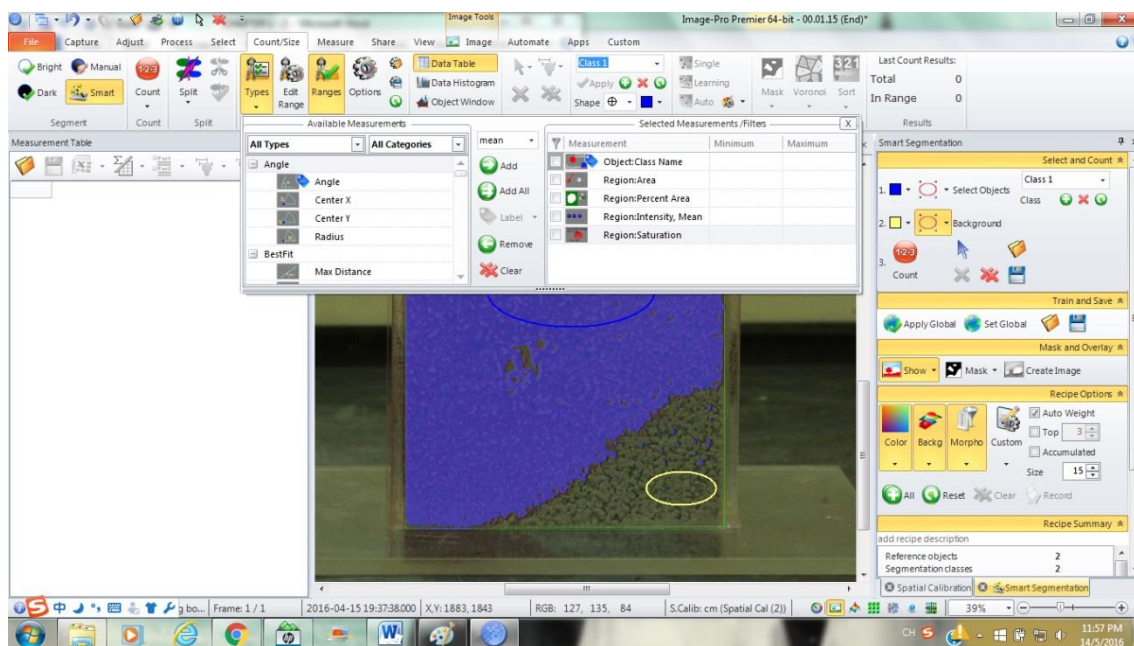
Figure 3.8: Selecting types of measurement
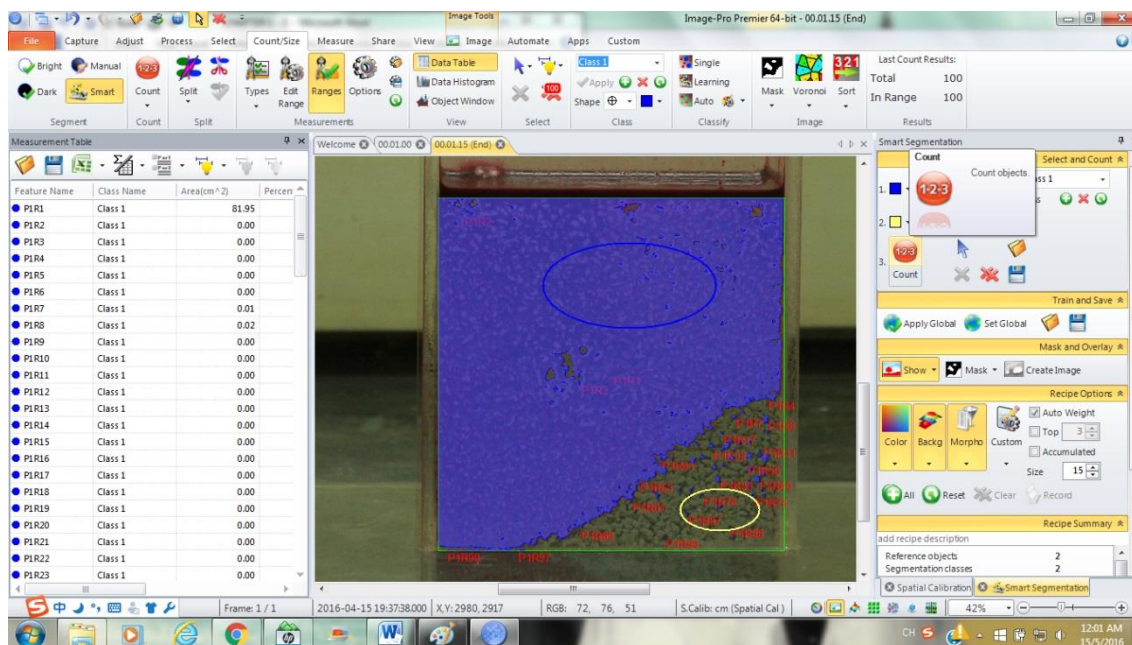
Figure 3.9: Generating analysis result

Lastly, the data of analysis was exported to *Microsoft Excel* by choosing the *Export* option in *Measurement Table* dialog as shown in Figure 3.10. Only the related data in each *Excel* sheet was selected to form a table of overall result when interpreting data.
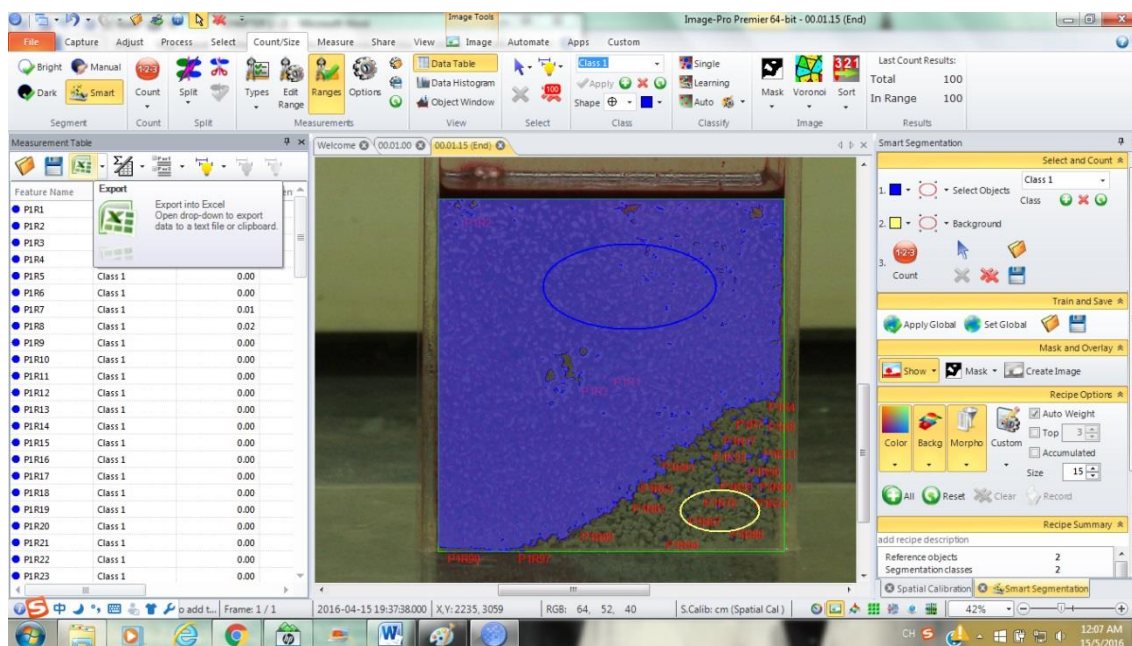
Figure 3.10: Exporting data to Microsoft Excel

CHAPTER 4

RESULTS AND DISCUSSIONS

4.1 PHYSICAL PROPERTIES OF SOIL SAMPLE

The results of physical properties tests for the soil sample will be discussed in the subsections below. The physical properties that have been determined are liquid limit, plastic limit, plasticity index, specific gravity, particle size distribution, classification of soil, permeability coefficient, specific surface area and porosity.

4.1.1 Liquid Limit

Clayey dry soil underwent distinct changes in consistency and behaviour when it was added with increasing amount of water. The moisture content at the point of transition from plastic to liquid state is the liquid limit. Due to difficulty in achieving the liquid limit from a single test, three tests were conducted at various moisture contents to determine the fall cone penetration, d. The data of fall cone test is shown in Appendix B. Liquid limit is corresponding to the moisture content at $d = 20$ mm. Referring to Figure 4.1, the liquid limit determined is 37.1 %.

4.1.2 Plastic Limit and Plasticity Index

The moisture content at the point of transition from semisolid to plastic state is the plastic limit. It is the lower limit of the plastic stage of soil. The data in obtaining plastic limit is shown in Appendix C. Using rolling method, it was determined that the plastic limit of sample in this research is 26.06 %. The plasticity index (*PI)* is the difference between the liquid limit and the plastic limit of a soil (Das & Sobhan, 2013).

Hence, the plasticity index of sample in this research is 11.04 % as calculated using Equation 4.1.

$$PI = LL - PL \hspace{4cm} (4.1)$$
$$PI = 37.1 - 26.06$$
$$= 11.04 \ \%$$
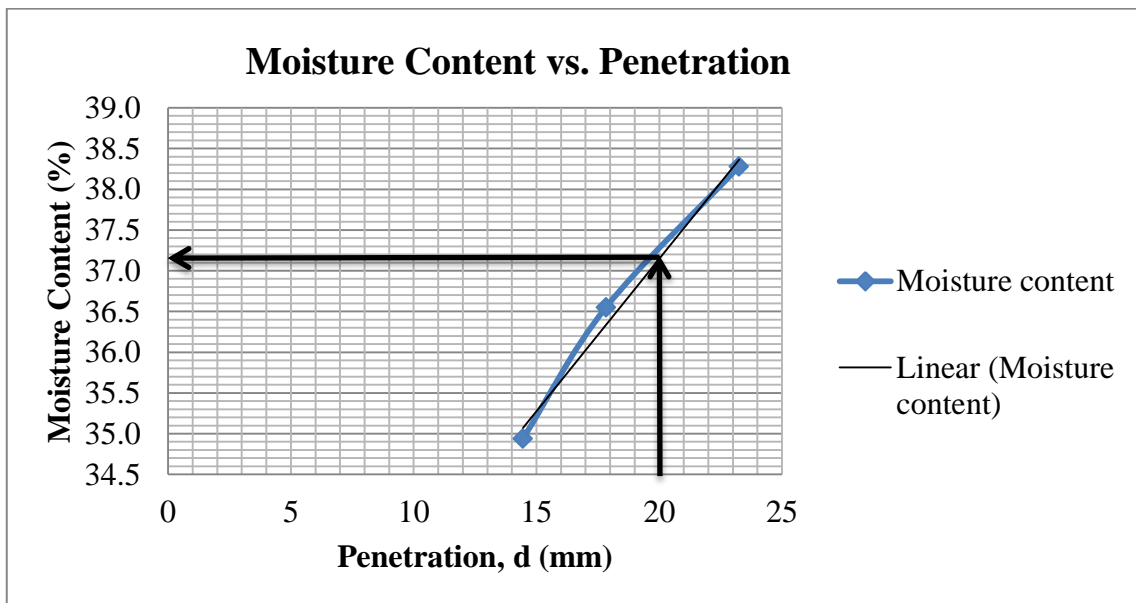
Figure 4.1: Graph of moisture content vs. cone penetration

4.1.3 Specific Gravity

Specific gravity is defined as the ratio of the unit weight of a material to the unit weight of water (Das and Sobhan, 2013). Using water pycnometer method, the specific gravity of sample in this research is 2.65. Appendix D shows the data in obtaining specific gravity. The specific gravity of sample was calculated using equation written in Appendix D.

4.1.4 Sieve Analysis

A soil is made up of soil particles with wide range of sizes. Soils generally are called gravel, sand, silt, or clay, depending on the pre-dominant size of particle within

the soil (Das & Sobhan, 2013). Sieve analysis was carried out to determine the distribution of the coarser soil particles. The calculations in determining the percent passing of soil sample are shown in Appendix E. The result obtained from sieve analysis is tabulated in Table 4.1.

Table 4.1: Result of sieve analysis

Sieve Size (mm)	Mass of sieve (g)	Mass retained on sieve + sieve (g)	Mass of soil retained (g)	Cumulative mass of soil (g)	Percent retained (%)	Percent passing (%)
4.750	407.620	407.620	0.000	0.000	0.000	100.000
2.360	534.950	535.050	0.100	0.100	0.052	99.948
1.180	485.770	486.110	0.340	0.440	0.229	99.771
0.600	483.850	484.350	0.500	0.940	0.489	99.511
0.300	448.110	448.360	0.250	1.190	0.618	99.382
0.212	439.670	439.890	0.220	1.410	0.733	99.267
0.150	423.170	432.070	8.900	10.310	5.358	94.642
0.063	257.680	304.180	46.500	56.810	29.524	70.476
Pan	532.010	667.200	135.190	$\sum M = 192.000$	100.000	0.000

4.1.5 Hydrometer Analysis

Hydrometer analysis was used to find out the distribution of finer soil particles. Based on the concept of Stoke's law, the percentage of silt and clay in inorganic fraction of soil can be obtained from the governing the rate of sedimentation of soil particles in water. The basic measurements and calculations in hydrometer analysis are shown in Appendix F. The result obtained from hydrometer analysis is tabulated in Table 4.2.

Table 4.2: Result of hydrometer analysis

Date	Time	Elapse time, t (minute)	Temperature, T (^{0}C)	Reading (R_h')	$R_h' + C_m$	Viscosity, η (mPa.S)	Effective depth, H_R (mm)	Particle diameter, D (mm)	R_d	% Finer than D (K %)
4/1/2016	9.30am	0.5	25.5	1.0150	1.0145	0.8817	139.1897	0.0675	0.0165	0.0530
		1	25.5	1.0140	1.0135	0.8817	143.2111	0.0484	0.0155	0.0498
		2	25.5	1.0130	1.0125	0.8817	147.2325	0.0347	0.0145	0.0466
		4	25.5	1.0105	1.0100	0.8817	157.2860	0.0254	0.0120	0.0385
		8	25.5	1.0080	1.0075	0.8817	167.3395	0.0185	0.0095	0.0305
		16	25.5	1.0065	1.0060	0.8817	173.3716	0.0133	0.0080	0.0257
		32	25.4	1.0050	1.0045	0.8836	179.4037	0.0096	0.0065	0.0209
		60	25.3	1.0040	1.0035	0.8854	183.4251	0.0071	0.0055	0.0177
		120	25.1	1.0030	1.0025	0.8891	187.4465	0.0051	0.0045	0.0145
		240	24.7	1.0025	1.0020	0.8977	189.4572	0.0036	0.0040	0.0128
		480	24.3	1.0020	1.0015	0.9065	191.4679	0.0026	0.0035	0.0112
5/1/2016	9.30am	1440	25.5	1.0010	1.0005	0.8817	195.4893	0.0015	0.0025	0.0080
6/1/2016	9.30am	2880	25.1	1.0007	1.0002	0.8891	196.6957	0.0011	0.0022	0.0071
7/1/2016	9.30am	4320	25.8	1.0005	1.0000	0.8761	197.5000	0.0009	0.0020	0.0064
8/1/2016	9.30am	5760	24.7	1.0005	1.0000	0.8977	197.5000	0.0008	0.0020	0.0064
11/1/2016	9.30am	10080	25.2	1.0005	1.0000	0.8873	197.5000	0.0006	0.0020	0.0064

4.1.6 Particle Size Distribution and Classification of Soil

Particle size distribution curve is drawn from the combination of results of sieve analysis and hydrometer analysis. The particle size distribution curve shows the range of particle size present in the soil sample and also the type of distribution of particles with different sizes. As shown in Figure 4.2, the soil sample is well-graded soil because the particle sizes are distributed over a wide range.
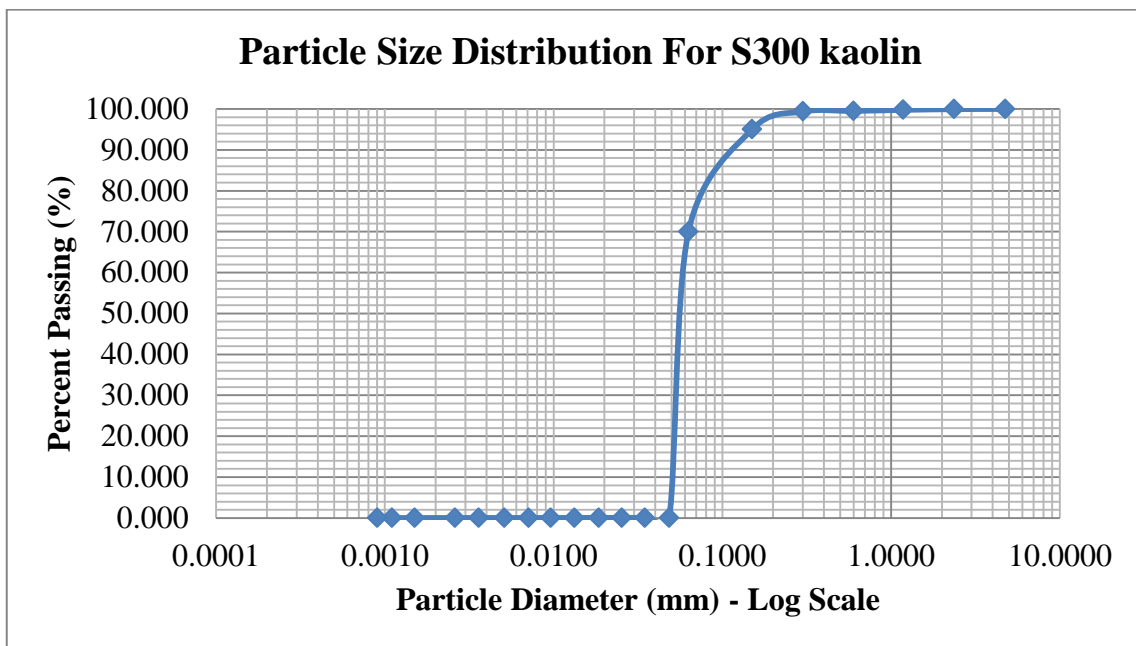
Figure 4.2: Particle size distribution curve

Three parameters for the soil sample are determined from the particle-size distribution curve:

i) Effective size, $D_{10} = 0.066$

ii) Uniformity coefficient, C_u

$$C_u = \frac{D_{60}}{D_{10}} \tag{4.2}$$

$$C_u = \frac{0.081}{0.066}$$

$$C_u = 1.227$$

iii)   Coefficient of gradation, *Cc*

$$C_c = \frac{D_{30}^2}{D_{60} \times D_{10}}$$ (4.3)

$$C_c = \frac{0.061^2}{0.081 \times 0.066}$$

$$= 0.696$$

Particle size distribution is taken into consideration when the sample is classified using Unified Soil Classification System (USCS). The particle-size distribution curve indicates the percent passing No. 200 sieve (0.075 mm) is more than 50 % and hence, the soil sample falls into the fine-grained soils category. In this category, the soil sample is silt and clay with liquid limit less than 50. The soil sample is further classified into group CL because its plasticity index is more than 7. Referring to ASTM D 2487, the group name of soil sample is sandy lean clay.

4.1.7   Permeability Coefficient

Falling head test was used to determine the coefficient of permeability of fine soil. As shown in Appendix G, the values of coefficient of permeability for the soil sample are 7.017×10^{-12}, 7.393×10^{-12}, 1.123×10^{-11} for T_1, T_2. T_3. Using equation in Appendix G, the permeability coefficient of sample used in this research is 8.543×10^{-12}. Referring to Appendix H, the soil sample is clay soil type with permeability less than 10^{-7}.

4.1.8   Specific Surface Area

The Brunauer-Emmelt-Teller technique is the most common method for determining the specific surface of soil material. Using this technique, nitrogen gas was employed as the probe molecule and was exposed to solid under investigation at liquid nitrogen condition. From the summary of report as attached in Appendix I, the single point surface area of soil sample at relative pressure is $1.8623 m^2/g$.

4.1.9 Porosity

Groundwater movement and storage occur in the pores of soil. Gas adsorption analysis is commonly used for porosity measurement. From the summary of report as attached in Appendix I, the single point adsorption total pore volume of pores less than 1, 425.568 Å width at relative pressure is 0.007173 cm^3/g.

4.2   MIGRATION BEHAVIOUR OF LNAPL IN AGGREGATED KAOLIN

The migration behaviour of LNAPL in aggregated kaolin were observed at four different moisture contents which are 27 %, 29 %, 31 % and 33 % respectively. The coverage area of LNAPL migration at the end of each experiment is displayed in Figure 4.3. The types of measurements generated from analysis for each sample are area, percent area, mean intensity and saturation. Comparison is made on area, rate of migration, velocity, mean intensity and saturation of LNAPL migration behaviour in aggregated kaolin of different moisture content.

4.2.1   Duration of LNAPL Migration

The data of migration behaviour of LNAPL in aggregated kaolin of 27 % moisture content is tabulated in Appendix J. It is shown in the appendix that the sample took 1 hr 35 mins to reach the bottom of flow chamber.

The data of migration behaviour of LNAPL in aggregated kaolin of 29 % moisture content is displayed in Appendix K. As shown in the appendix, the sample took lesser time, which is 42 mins to migrate downwards to the bottom of flow chamber compared to sample of 27 % moisture content.

The data of migration behaviour of LNAPL in aggregated kaolin of 31 % moisture content is shown in Appendix L and it shows that the sample took only 1 min 15 s to flow towards the base of flow chamber. This shows that the duration of LNAPL migration becomes shorter as the moisture content increases from 27 % to 31 %. The

result is supported by the observation from research carried out by Sa'ari et al. (2015) where inter-aggregate pores of soil sample with higher moisture content is larger and LNAPL tends to move downward faster.

However, the data in Appendix M shows that the migration of LNAPL is slower in sample of 33 % moisture content than that of the sample of 31% moisture content. From the appendix, it is shown that the LNAPL in aggregated kaolin of 33% moisture content took a total duration of 8 mins to reach the bottom of flow chamber. The optimality of double-porosity condition for the aggregated kaolin may cause the change of pattern in result which the duration of LNAPL migration increased instead of decreased from 31 % moisture content.
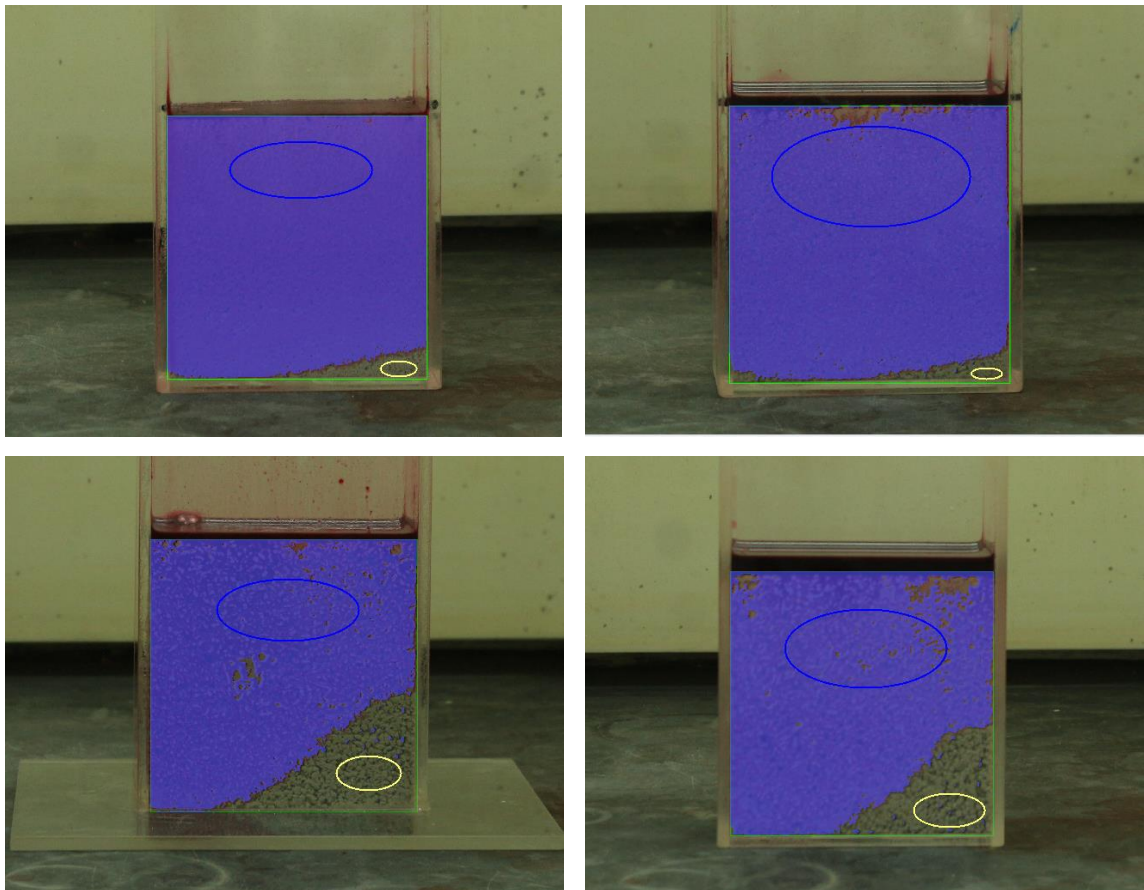
Figure 4.3 (from top left): The area coverage of LNAPL migration in aggregated kaolin of 27 %, 29 %, 31 % and 33 % respectively

4.2.2 Comparison on Area of LNAPL Migration

Comparison on area of LNAPL migration at different moisture content of aggregated kaolin versus time is established in line graph as shown in Figure 4.4. From the graph, it is obviously shown that the area of LNAPL migration in sample of 31 % moisture content is the smallest which is 87.033 cm^2 compared to samples of 27 %, 29 % and 33 % moisture content which the areas are 97.739 cm^2, 98.832 cm^2 and 91.766 cm^2 respectively.

From the finding of Sa'ari et al. (2015), higher moisture content resulted in larger inter-aggregate pores. Hence, it can be proven that the inter-aggregate pores of sample with 31 % moisture content is larger than that of samples of 27 % and 29 % moisture contents. The larger the pores size of the sample, the more the amount of trapped residual LNAPL in the pores. The amount of LNAPL migrate downwards to the bottom of flow chamber decreases when the amount of trapped residual LNAPL in pores increases, thus, the area of LNAPL migration also decreases.
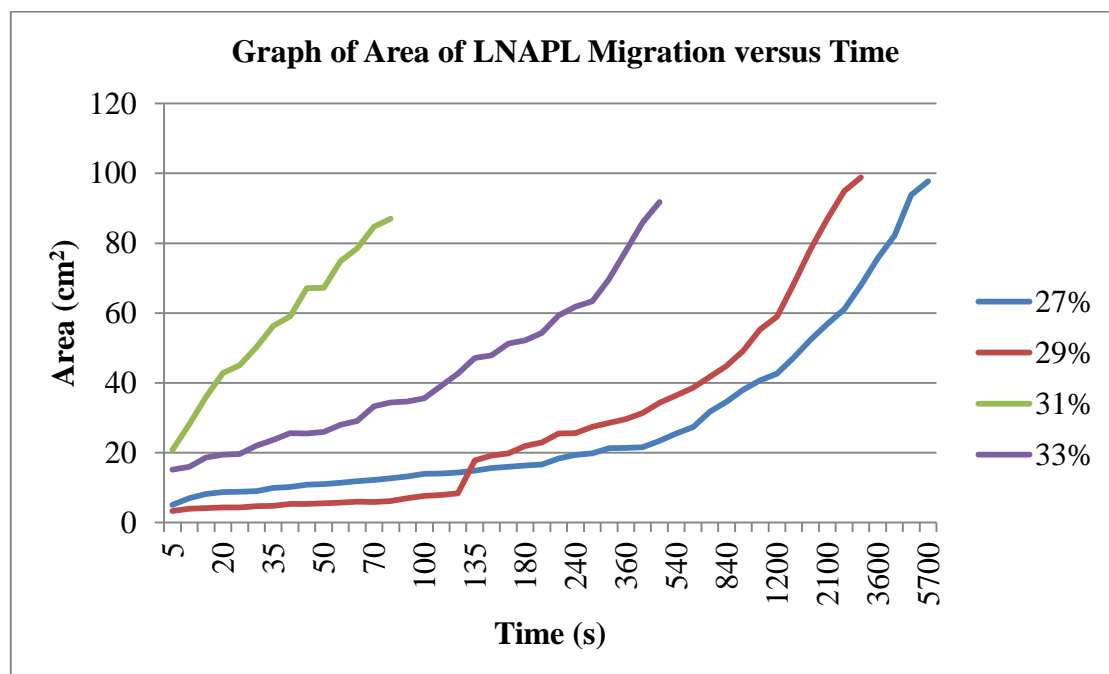
Figure 4.4: Area of LNAPL migration vs. time in aggregated kaolin of 27 %, 29 %, 31 % and 33 % moisture contents

The area of LNAPL migration in sample of 33 % moisture content is smaller than that of sample 31 % moisture content because 31 % moisture content may not be an ideal condition of double porosity to investigate the LNAPL migration in this research. Hence, the pattern of result for sample of 33 % differs from the pattern of result in 27 %, 29 % and 31 % moisture content.

The rate of migration of LNAPL is obtained using Equation 4.4.

$$\text{Rate of Migration} = \frac{Total\ Area\ of\ LNAPL\ Migration}{Total\ Duration\ of\ LNAPL\ Migration} \qquad (4.4)$$

The rate of LNAPL migration in aggregated kaolin of different moisture contents is shown in Table 4.3. The rates of LNAPL migration are 0.017 cm^2/s, 0.039 cm^2/s, 1.087 cm^2/s and 0.191 cm^2/s in aggregated kaolin of 27 %, 29 %, 31 % and 33 % respectively. Aggregated kaolin of 31 % moisture content has the faster rate of LNAPL migration as compared to aggregated kaolin of 27 % and 29 % moisture content. This is due to the higher moisture content which leads to larger pore size. This explanation is proven by the research conducted by Sa'ari et al. (2015) that LNAPL moved downward faster when the moisture content increased. Capillary pressure decreases with increasing pore size. Therefore, the movement of LNAPL is less restricted by weaker capillary pressure in 31 % moisture content due to the larger inter-aggregate pores of soil sample.

Table 4.3: Rate of LNAPL Migration

Moisture Content of Sample (%)	Total Area of LNAPL Migration (cm^2)	Total Duration of LNAPL Migration (s)	Rate of LNAPL Migration (cm^2/s)
27	97.739	5700	0.017
29	98.832	2520	0.039
31	87.033	80	1.087
33	91.766	480	0.191

4.2.3 Comparison on Velocity of LNAPL Migration

The velocity of LNAPL migration is obtained using Equation 4.5.

$$\text{Velocity of Migration} = \frac{Total\ Depth\ of\ LNAPL\ Migration}{Total\ Duration\ of\ LNAPL\ Migration} \qquad (4.5)$$

The velocity of LNAPL migration in aggregated kaolin of different moisture content is shown in Table 4.4. LNAPL in sample of 31 % travelled with the highest velocity which is 0.013 cm/s as compared to the other samples. The velocity of LNAPL migration in sample of 27 %, 29 % and 33 % are 0.002 cm/s, 0.004 cm/s and 0.021 cm/s respectively. The velocity of LNAPL migration in sample of 31 % moisture content is the highest due to the weaker capillary pressure exerted in the pores of sample at higher moisture content. When the capillary pressure is minimized, the LNAPL flows with greater speed and reach the bottom of flow chamber at a faster rate and hence, resulted in highest velocity of migration.

Table 4.4: Velocity of LNAPL Migration

Moisture Content of Sample (%)	Total Depth of LNAPL Migration (cm)	Total Duration of LNAPL Migration (s)	Velocity of LNAPL Migration (cm/s)
27	10	5700	0.002
29	10	2520	0.004
31	10	80	0.013
33	10	480	0.021

4.2.4 Comparison on Mean Intensity of LNAPL Migration

Colours have scales. The scale of colour used in the analysis of this research is hue, saturation and intensity. Intensity is used to describe the lightness of LNAPL colour in image analysis of this research. It defines a range from dark (0 %) to fully

illuminated (100 %). The intensity of the colour is influenced by the energy output of artificial light source during the experiment.

Comparison on the mean intensity of LNAPL migration in aggregated kaolin with different moisture content is shown in Figure 4.5. The mean intensity of LNAPL varies throughout the experiment of each sample because intensity changes when the amount of light reflected on the flow chamber changes. The highest mean intensity of LNAPL in sample of 27 % moisture content is 85.123 lm while the lowest intensity is 51.034 lm. For sample of 29 % moisture content, the highest mean intensity of LNAPL is 63.221 lm while the lowest mean intensity is 46.390 lm. The range of mean intensity of LNAPL in sample of 31 % moisture content varies within the range of 25 to 40 lm with the highest is 37.065 lm while the lowest is 28.666 lm. On the other hand, LNAPL in sample of 33 % moisture content has the highest mean intensity of 65.550 lm and the lowest mean intensity of 52.073 lm.

Combining the mean intensity of four samples, the mean intensity is in the range of 25 to 90 lm in this research. It can be observed from the bar chart in Figure 4.4 that the mean intensity of LNAPL is more uniform in sample of 31 % moisture content with shortest duration of LNAPL migration. The shorter the duration of LNAPL migration, the lesser the variation of mean intensity throughout the experiment. The non-uniformity of mean intensity for the other three samples which are of 27 %, 29 % and 33 % maybe caused by the external factor such as the opening and closing of door that let in other light source such as sunlight when other personnel accessed the laboratory. Furthermore, it may be caused by the obstruction of light source when other individuals were working in the laboratory.

4.2.5   Comparison on Saturation of LNAPL Migration

Hue is qualitative. It is used to describe the basic colour in terms of green, red and blue. On the other hand, saturation refers to the purity of a hue from grey tone (no saturation) to pure colour (high saturation). Using analysis of software, the saturation data is used to study the relative fraction of total pore space containing LNAPL in aggregated kaolin. This is evidently support by the investigation of the implication of

image upscaling on saturation distribution (Christ et al., 2012) that proved that image averaging had negligible influence on the average saturation.

Comparison on the saturation of LNAPL migration in aggregated kaolin of different moisture content is established in bar chart as shown in Figure 4.6. As shown in Figure 4.6, the final saturation of LNAPL migration in samples of 27 %, 29, and 31 % moisture content are 54.644 lm, 41.516 lm and 33.594 lm respectively. Residual saturation of LNAPL represents the LNAPL that is tightly held in the pore spaces. From the review of Mercer & Cohen (1990), the residual saturation of most NAPLs ranged about 10 % to 20 % in the unsaturated zone. The saturation of LNAPL migration decreases with increasing moisture content from 27 % to 31 %. This may be due to the increasing pore sizes of the sample as the moisture content increases. At higher moisture contents, the pore size is larger and thus the residual saturation of LNAPL is higher.

From Figure 4.6, the final saturation of LNAPL migration is 39.304 lm in sample of 33 % moisture content. Due to the reason that 33 % moisture content is not an optimum condition for double-porosity properties of aggregated kaolin, the final saturation of LNAPL migration is higher than that of sample of 31 % moisture content.

Figure 4.5: Mean Intensity of LNAPL migration vs. time in aggregated kaolin of 27 %, 29 %, 31 % and 33 % moisture contents

Figure 4.6: Saturation of LNAPL migration vs. time in aggregated kaolin of 27 %, 29 %, 31 % and 33 % moisture contents
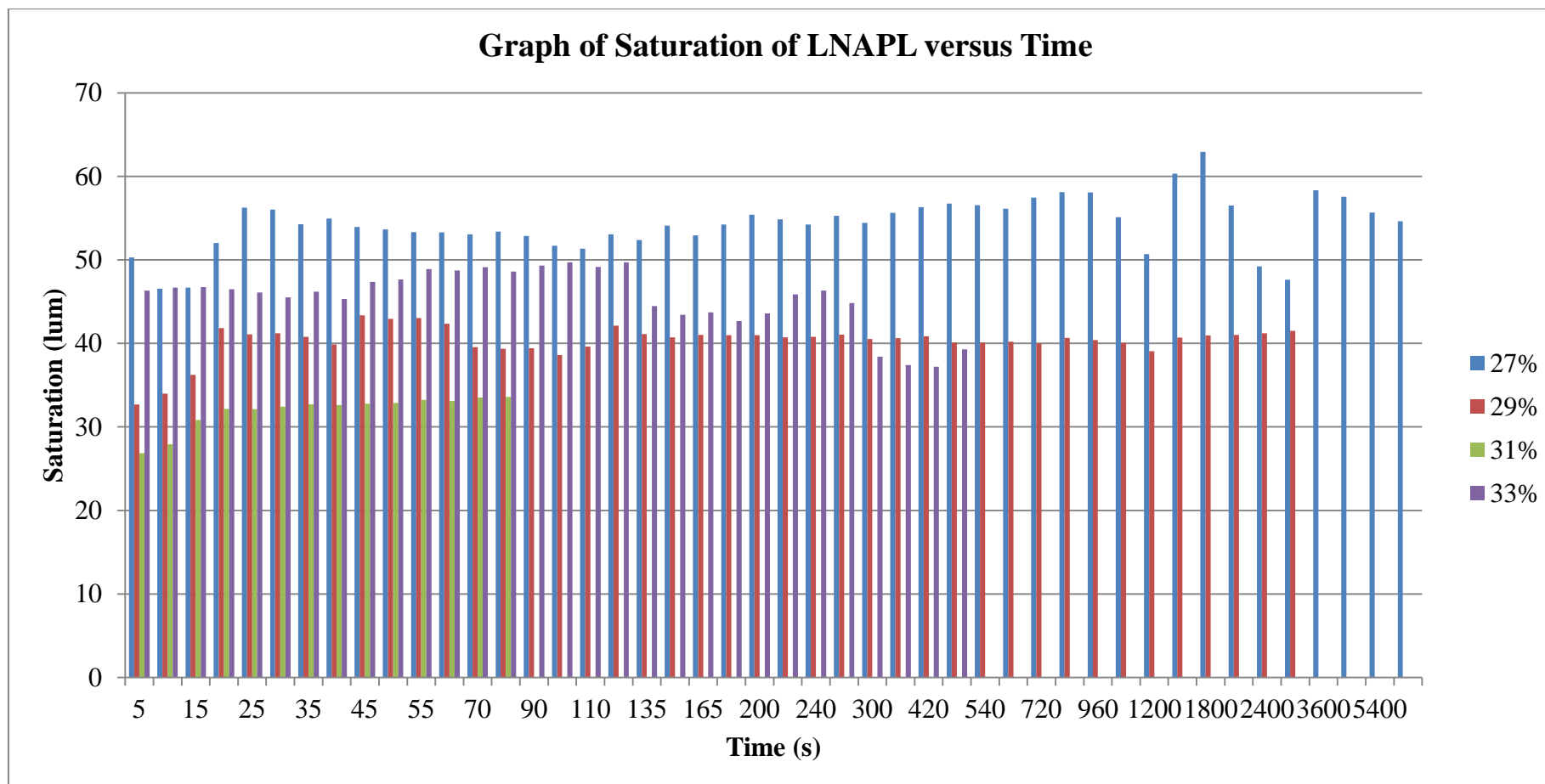
CHAPTER 5

CONCLUSIONS AND RECOMMENDATIONS

5.1   CONCLUSIONS

Some physical properties tests of soil sample were carried out in this research. However, the main concern of this research was the laboratory experiment on the effect of different moisture of aggregated kaolin in migration behaviour of LNAPL using Light Reflection Method. The data of experiment was analysed using Image-Pro Premier 9.1. Based on the result obtained, the objectives of research were achieved and several conclusions were made.

i)   The migration behaviour of LNAPL in double porosity media were observed using aggregated kaolin of 27 %, 29 % and 31 % moisture content. In addition, 33 % moisture content was not an ideal condition to form double porosity media.

ii)   The rate of LNAPL migration in aggregated kaolin was influenced by the different moisture content of soil sample. Within the optimum range, the higher the moisture content of soil sample, the higher the rate of LNAPL migration.

iii) The area of LNAPL migration in aggregated kaolin was affected by the different moisture content of soil sample. Within the range of ideal moisture content, the area of soil sample contaminated by LNAPL was larger as the moisture content of soil sample was higher.

iv) Image-Pro Premier 9.1 is a simple and handy tool that was used to analyse experiment data. It converted the experiment data into hue, saturation and intensity format to ease interpretation of data. Data of saturation and intensity of LNAPL migration were generated from the software analysis.

5.2 RECOMMENDATIONS

Research was carried out on the effect of different moisture content on the migration behaviour of aggregated kaolin using Light Reflection Method. Based on the experiment outcome, several recommendations were made for further improvement in future research study.

i) Dry kaolin should be mixed evenly with the water at the shortest duration possible during sample preparation to avoid excessive moisture content loss. This can also be further improved by preparing the sample at a place with low wind exposure to reduce the evaporation rate of sample.

ii) The flow chamber should be placed at a position far away from building access such as door and windows to maintain consistency on the intensity of light during experiment. The light that penetrates through the door gap and windows can affect the amount of light reflected on the flow chamber and leads to the inconsistency of intensity.

iii) Camera mounted on tripod should be in static condition without external disturbance during the experiment. This is to assure the accuracy of experiment result in order to produce an accurate analysis.

iv) When conducting fall cone penetration test, the soil sample in metal cup should be knocked not more than thrice to reduce voids and avoid excessive compaction which can make the soil sample to liquefy easily on the surface.

REFERENCES

American Society of the International Association for Testing and Materials (2002) D422-63: *Standard Test Method for Particle-Size Analysis of Soils*

American Society of the International Association for Testing and Materials (2002) D854-02: *Standard Test Methods for Specific Gravity of Soil Solids by Water Pycnometer*

American Society of the International Association for Testing and Materials (2000) D2487-00: *Standard Practice for Classification of Soils for Engineering Purpose (Unified Soil Classification System)*

American Society of the International Association for Testing and Materials (2000) D4318-00: *Standard Test Methods for Liquid Limit, Plastic Limit, and Plasticity Index of Soils*

American Society of the International Association for Testing and Materials (2013) D4567-03: *Standard Test Methods for Single-Point Determination of Specific Surfaace Area of Catalysts and Catalyst Carrieers Using Nitrogen Adsorption by Continuous Flow Method*

American Society of the International Association for Testing and Materials (2012) D4641-12: *Standard Practice for Calculation of Pore Size Distributions of Catalysts and Catalyst Carriers from Nitrogen Desorption Isotherms*

American Society of the International Association for Testing and Materials (2004) D5084-03: *Standard Test Methods for Measurement of Hydraulic Conductivity of Saturated Porous Materials Using a Flexible Wall Permeameter*

Borzooei, S., Reddy, E.S. and Reddy, G.N., 2014. An experimental study about influence of viscosity of fluid on spread of contaminant in sand deposits.

Christ, J.A., Pennell, K.D. and Abriola, L.M., 2012. Quantification of experimental subsurface fluid saturations from high-resolution source zone images. *Water Resources Research*, *48*(1).

Das. B., & Sobhan, K. (2013). *Principles of geotechnical engineering*. Cengage Learning.

Kamaruddin, S.A., Sulaiman, W.N.A., Zakaria, M.P., Othman, R. and Rahman, N.A., 2011, September. Laboratory simulation of LNAPL spills and remediation in unsaturated porous media using the image analysis technique: A review. In *National Postgraduate Conference (NPC), 2011* (pp. 1-7). IEEE.

Katsifarakis, K. L. (Ed.). (2000). *Groundwater Pollution Control*. Wit Press.

Ladd, J.N., Foster, R.C., Nannipieri, P. and Oades, J.M., 1996. Soil structure and biological activity. *Soil biochemistry*, *9*, pp.23-78.

Mercer, J.W. and Cohen, R.M., 1990. A review of immiscible fluids in the subsurface: properties, models, characterization and remediation. *Journal of Contaminant Hydrology*, *6*(2), pp.107-163.

Newell, C.J., Acree, S.D., Ross, R.R. and Huling, S.G., 1995. *Ground water issue: light nonaqueous phase liquids* (No. PB--95-267738/XAB). Groundwater Services, Inc., Houston, TX (United States).

Oostrom, M., Dane, J.H. and Wietsma, T.W., 2006. A review of multidimensional, multifluid intermediate-scale experiments. *Vadose Zone Journal*, *5*(2), pp.570-598.

Ramaswami, A., Milford, J.B. and Small, M.J., 2005. *Integrated environmental modeling: pollutant transport, fate, and risk in the environment*. J. Wiley.

Sa'ari, R., Rahman, N.A., Yusof, Z.M., Ngien, S.K., Kamaruddin, S.A., Mustaffar, M. and Hezmi, M.A., 2015. Application Of Digital Image Processing Technique In Monitoring LNAPL Migration In Double Porosity Soil Column. *Jurnal Teknologi*, *72*(3).

Sharma, H.D. and Reddy, K.R., 2004. *Geoenvironmental engineering: site remediation, waste containment, and emerging waste management technologies*. John Wiley & Sons, Inc..

Weiner, R. and Matthews, R. eds., 2003. *Environmental engineering*. Butterworth-Heinemann.

Werth, C.J., Zhang, C., Brusseau, M.L., Oostrom, M. and Baumann, T., 2010. A review of non-invasive imaging methods and applications in contaminant hydrogeology research. *Journal of contaminant hydrology*, *113*(1), pp.1-24.

APPENDIX A

MSDS No: M01106

MATERIAL SAFETY DATA SHEET

1. CHEMICAL PRODUCT AND COMPANY IDENTIFICATION

Product Name: Toluene
Catalog Number: 1447017

Hach Company
P.O.Box 389
Loveland, CO USA 80539
(970) 669-3050

Emergency Telephone Numbers:
(Medical and Transportation)
(303) 623-5716   24 Hour Service
(515)232-2533   8am - 4pm CST

MSDS Number: M01106
Chemical Name: Benzene, methyl-
CAS No.: 108-88-3
Chemical Formula: C_7H_8
Chemical Family: Aromatic Compounds
Hazard: Causes irritation. Flammable. Harmful if swallowed, inhaled or absorbed through skin.
Date of MSDS Preparation:
  Day: 04
  Month: December
  Year: 2007

2. COMPOSITION / INFORMATION ON INGREDIENTS

Toluene
  CAS No.: 108-88-3
  TSCA CAS Number: 108-88-3
  Percent Range: 100.0
  Percent Range Units: volume / volume
  LD50: Oral rat LD50 = 636 mg/kg
  LC50: Inhalation rat LC50 = 49 $g/m^3/4H$, Inhalation mouse LC50 = 400 ppm/24H
  TLV: 50 ppm
  PEL: TWA = 200 ppm; celling = 300 ppm
  Hazard: Causes irritation. Flammable. Harmful if swallowed, inhaled or absorbed through skin.

3. HAZARDS IDENTIFICATION

Emergency Overview:
  Appearance: Clear, colorless liquid
  Odor: Benzene-like
    HARMFUL OR FATAL IF SWALLOWED HARMFUL IF INHALED OR ABSORBED THROUGH
  SKIN VAPOR HARMFUL CAUSES EYE IRRITATION MAY CAUSE SKIN AND RESPIRATORY
  TRACT IRRITATION

    FLAMMABLE LIQUID AND VAPOR

HMIS:
  Health: 2

APPENDIX A (Continued)

Flammability: 4
Reactivity: 0
Protective Equipment: X - See protective equipment, Section 8.
NFPA:
  Health: 2
  Flammability: 3
  Reactivity: 0
  Symbol: Not applicable
Potential Health Effects:
  Eye Contact: Causes severe irritation
  Skin Contact: Can defat the skin causing: skin redness, irritation or dermatitis Causes moderate irritation
  Skin Absorption: Will be absorbed through the skin. Effects similar to those of ingestion
    Target Organs: Central nervous system Liver Bone marrow
  Ingestion: May be fatal if swallowed May cause: irritation of the mouth and esophagus metallic taste salivation coughing gastrointestinal disturbances nausea vomiting loss of appetite central nervous system effects slow reaction times hallucinations incoordination giddiness confusion stupor vertigo ringing in the ears (tinnitus) coma blood changes anemia bone marrow changes Can cause: enlarged liver narcotic effects
    Target Organs: Central nervous system Liver Bone marrow
  Inhalation: Causes: respiratory tract irritation Effects similar to those of ingestion.
    Target Organs: Central nervous system Liver Bone marrow
  Medical Conditions Aggravated: Eye conditions Dermatitis Liver conditions Respiratory conditions Cardiovascular diseases
  Chronic Effects: Chronic overexposure may cause weakness paralysis low levels of potassium in the blood gastrointestinal disturbances abdominal pain nausea vomiting central nervous system effects headache dizziness lethargy hallucinations coma
  Cancer / Reproductive Toxicity Information:
    O.S.H.A. Listed: No

    IARC Listed: No

    NTP Listed: No

    Additional Cancer / Reproductive Toxicity Information: an experimental teratogen.
  Toxicologically Synergistic Products: None reported

4. FIRST AID

Eye Contact: Immediately flush eyes with water for 15 minutes. Call physician immediately.
Skin Contact (First Aid): Wash skin with soap and plenty of water for 15 minutes. Call physician immediately.
Ingestion (First Aid): Do not induce vomiting. Call physician immediately.
Inhalation: Remove to fresh air. Give artificial respiration if necessary. Call physician.

5. FIRE FIGHTING MEASURES

Flammable Properties: Flammable Liquid Vaporizes easily at normal temperatures. Vapors can travel to a source of ignition and flash back.
Flash Point: 4.4° C (40° F)
Method: Closed cup
Flammability Limits:
  Lower Explosion Limits: 1.4%
  Upper Explosion Limits: 6.7%
Autoignition Temperature: 536° C (997° F)
Hazardous Combustion Products: carbon monoxide, carbon dioxide.

APPENDIX A (Continued)

Fire / Explosion Hazards: May explode on contact with: nitric acid nitric acid + sulfuric acid + heat bromine trifluoride May ignite on contact with: heat sparks, flame, or other ignition sources May form explosive mixtures with: nitromethane May react violently with: oxidizers

   Static Discharge: None reported.

   Mechanical Impact: None reported

Extinguishing Media: Alcohol foam. Carbon dioxide Dry chemical.

Fire Fighting Instruction: As in any fire, wear self-contained breathing apparatus pressure-demand and full protective gear. Containers can build up pressure if exposed to heat.

6. ACCIDENTAL RELEASE MEASURES

Spill Response Notice:

   Only persons properly qualified to respond to an emergency involving hazardous substances may respond to a spill according to federal regulations (OSHA 29 CFR 1910.120(a)(v)) and per your company's emergency response plan and guidelines/procedures. See Section 13, Special Instructions for disposal assistance.

Containment Technique: Releases of this material may contaminate the environment. Remove all combustible material from spill area. Remove all ignition and spark-creating sources from the spill area. Cover spilled liquid with a commercially available flammable liquid sorbent such as vapor barrier blanket or activated carbon to avoid evolution of fumes. Vapors may travel to a source of ignition and flash back. May be ignited by: heat, sparks, or flames. Material will float on water creating a fire hazard. Dike the material to create a barrier to combustibles.

Clean-up Technique: Eliminate all sources of ignition. Do not breathe the fumes. Cover with an inert material, such as sand. Use only non-sparking tools. Sweep up material. Incinerate material at an E.P.A. approved hazardous waste facility. Decontaminate the area of the spill with a soap solution.

Evacuation Procedure: Evacuate general area (50 foot radius or as directed by your facility's emergency response plan) when: any quantity is spilled. If conditions warrant, increase the size of the evacuation.

Special Instructions (for accidental release): Product is regulated as RCRA hazardous waste. Product is regulated as a hazardous air pollutant. Product is regulated as a hazardous water pollutant.

304 EHS RQ (40 CFR 355): Not applicable

D.O.T. Emergency Response Guide Number: 130

7. HANDLING / STORAGE

Handling: Avoid contact with eyes skin clothing Do not breathe mist or vapors. Wash thoroughly after handling. Use with adequate ventilation. Maintain general industrial hygiene practices when using this product.

Storage: Protect from: heat Keep away from: sparks, flames and other ignition sources oxidizers

   Flammability Class: Class IB

8. EXPOSURE CONTROLS / PROTECTIVE EQUIPMENT

Engineering Controls: Have an eyewash station nearby. Have a safety shower nearby. Maintain general industrial hygiene practices when using this product. Maintain adequate ventilation to keep vapor level below TWA for chemicals in this product.

Personal Protective Equipment:

   Eye Protection: chemical splash goggles

   Skin Protection: nitrile gloves

   Inhalation Protection: laboratory fume hood

Precautionary Measures: Avoid contact with: eyes skin clothing Do not breathe: mist/vapor Wash thoroughly after handling. Use with adequate ventilation. Protect from: heat Keep away from: sparks, flames and other ignition sources oxidizers

TLV: 50 ppm

PEL: TWA = 200 ppm; celling = 300 ppm

9. PHYSICAL / CHEMICAL PROPERTIES

Appearance: Clear, colorless liquid
Physical State: Liquid
Molecular Weight: 92.15
Odor: Benzene-like
pH: Not applicable
Vapor Pressure: 28.5 mm Hg @20° C
Vapor Density (air = 1): 3.1
Boiling Point: 111° C   (232° F)
Melting Point: -95° C   (-138° F)
Specific Gravity (water = 1): 0.866
Evaporation Rate (water = 1): 1.8
Volatile Organic Compounds Content: 100%
Partition Coefficient (n-octanol / water): log K_{0w} = 2.69
Solubility:
  Water: Slighlty soluble
  Acid: Soluble in glacial acetic
  Other: Soluble in petroleum ether, alcohol, chloroform, ether, acetone, carbon disulfide, acetate, benzene
Metal Corrosivity:
  Steel: Not determined
  Aluminum: None determined

10. STABILITY / REACTIVITY

Chemical Stability: Stable when stored under proper conditions.
Conditions to Avoid: Contact with heat, sparks, open flames or other ignition sources.
Reactivity / Incompatibility: May explode in contact with: nitric acid bromine trifluoride May react violently in contact with: oxidizers strong acids perchlorates nitrogen tetroxide
Hazardous Decomposition: Heating to decomposition releases: carbon dioxide carbon monoxide
Hazardous Polymerization: Will not occur.

11. TOXICOLOGICAL INFORMATION

Product Toxicological Data:
  LD50: Oral rat LD50 = 636 mg/kg
  LC50: Inhalation rat LC50 = 49 g/m^3/4H, Inhalation mouse LC50 = 400 ppm/24H
  Dermal Toxicity Data: Dermal rabbit LD50 = 14100 µg/kg
  Skin and Eye Irritation Data: Eye: rabbit 2 mg/24H - SEVERE; Skin: rabbit 20 mg/24H - MODERATE
  Mutation Data: DNA damage rat liver 30 µmol/l, Cytogenetic analysis Inhalation rat 5400 µg/m^3/16W (intermittent)
  Reproductive Effects Data: Inhalation rat TCLo = 1000 mg/m^3/24H Specific developmental abnormalities - musculoskeletal, Inhalation rat TCLo = 800 mg/m^3/6H Effects on embryo or fetus - fetotoxicity, Oral mouse TDLo = 9 g/kg fetal death
Ingredient Toxicological Data: --
Not applicable

12. ECOLOGICAL INFORMATION

Product Ecological Information: Bluegill LC50 = 17 mg/l/24H & 13 mg/l/96H, Grass Shrimp LC50 = 9.5 ppm/96H, Fathead minnow LC50 = 56 mg/l/24H & 34 mg/l/96H, Guppy LC50 = 59.3 mg/l/96H; Bioconcentration: mussel 4.2, algae 380, golden ide fish 90.

Ingredient Ecological Information: --

APPENDIX A (Continued)

Not applicable

---

13. DISPOSAL CONSIDERATIONS

EPA Waste ID Number: U220
Special Instructions (Disposal): Incinerate material at an E.P.A. approved hazardous waste facility.
Empty Containers: Rinse three times with an appropriate solvent. Rinsate from empty containers may contain sufficient product to require disposal as hazardous waste. Dispose of empty container as normal trash.
NOTICE (Disposal): These disposal guidelines are based on federal regulations and may be superseded by more stringent state or local requirements. Please consult your local environmental regulators for more information.

---

14. TRANSPORT INFORMATION

D.O.T.:
  D.O.T. Proper Shipping Name: Toluene
  --
  DOT Hazard Class: 3
  DOT Subsidiary Risk: NA
  DOT ID Number: UN1294
  DOT Packing Group: II
I.C.A.O.:
  I.C.A.O. Proper Shipping Name: Toluene
  --
  ICAO Hazard Class: 3
  ICAO Subsidiary Risk: NA
  ICAO ID Number: UN1294
  ICAO Packing Group: II
I.M.O.:
  I.M.O. Proper Shipping Name: Toluene
  --
  I.M.O. Hazard Class: 3
  I.M.O. Subsidiary Risk: NA
  I.M.O. ID Number: UN1294
  I.M.O. Packing Group: II
Additional Information: There is a possibility that this product could be contained in a reagent set or kit composed of various compatible dangerous goods. If the item is NOT in a set or kit, the classification given above applies. If the item IS part of a set or kit, the classification would change to the following: UN3316 Chemical Kit, Class 9, PG II or III. If the item is not regulated, the Chemical Kit classification does not apply.

---

15. REGULATORY INFORMATION

U.S. Federal Regulations:
  O.S.H.A.: This product meets the criteria for a hazardous substance as defined in the Hazard Communication Standard. (29 CFR 1910.1200)
  E.P.A.:
    S.A.R.A. Title III Section 311/312 Categorization (40 CFR 370): Immediate (Acute) Health Hazard Delayed (Chronic) Health Hazard Fire Hazard
    S.A.R.A. Title III Section 313 (40 CFR 372): This product contains a chemical(s) subject to the reporting requirements of Section 313 of Title III of SARA.
     Toluene
    302 (EHS) TPQ (40 CFR 355): Not applicable
    304 CERCLA RQ (40 CFR 302.4): 1000 lbs. Toluene
    304 EHS RQ (40 CFR 355): Not applicable
    Clean Water Act (40 CFR 116.4): Toluene - RQ 1000 lbs.

APPENDIX A (Continued)

RCRA: Contains RCRA regulated substances. See Section 13, EPA Waste ID Number.
C.P.S.C.: The label for this product bears the signal word "DANGER" and the words "HARMFUL OR FATAL IF SWALLOWED" and "VAPOR HARMFUL" because the Toluene concentration is greater than 10%
State Regulations:
  California Prop. 65: WARNING - This product contains a chemical known to the State of California to cause birth defects or other reproductive harm.
    Identification of Prop. 65 Ingredient(s): Toluene
  California Perchlorate Rule CCR Title 22 Chap 33:
Trade Secret Registry: Not applicable
National Inventories:
  U.S. Inventory Status: TSCA Listed: Yes
    TSCA CAS Number: 108-88-3

16. OTHER INFORMATION

Intended Use: Solvent
References: Air Contaminants, Federal Register, Vol. 54, No. 12. Thursday, January 19, 1989. pp. 2332-2983. CCINFO RTECS. Canadian Centre for Occupational Health and Safety. Hamilton, Ontario Canada: 30 June 1993. Fire Protection Guide on Hazardous Materials, 10th Ed. Quincy, MA: National Fire Protection Fire Protection Guide on Hazardous Materials, 10th Ed. Quincy, MA: National Fire Protection Association, 1991. Gosselin, R. E. et al. Clinical Toxicology of Commercial Products, 5th Ed. Baltimore: The Williams and Wilkins Co., 1984. In-house information. Patty, Frank A. Industrial Hygiene and Toxicology, 3rd Revised Edition. Volume 2. New York: A Wiley-Interscience Publication, 1981. Prager, Jan C. Environmental Contaminants Reference Databook, Volumes I and II. Van Nostrand Reinhold Company, New York. Sax, N. Irving and Richard J. Lewis, Sr., revised by. Hawley's Condensed Chemical Dictionary, Eleventh Ed. New York: Van Nostrand Reinhold Co., 1987. Sax, N. Irving. Dangerous Properties of Industrial Materials, 7th Ed. New York: Van Nostrand Reinhold Co., 1989. Technical Judgment. The Merck Index, 11th Ed. Rahway, New Jersey: Merck and Co., Inc., 1989. TLV's Threshold Limit Values and Biological Exposure Indices for 1992-1993. American Conference of Governmental Industrial Hygienists, 1992. Vendor Information.
Revision Summary: Updates in Section(s) 14,

Legend:

NA - Not Applicable	w/w - weight/weight
ND - Not Determined	w/v - weight/volume
NV - Not Available	v/v - volume/volume

USER RESPONSIBILITY: Each user should read and understand this information and incorporate it in individual site safety programs in accordance with applicable hazard communication standards and regulations.

THE INFORMATION CONTAINED HEREIN IS BASED ON DATA CONSIDERED TO BE ACCURATE. HOWEVER, NO WARRANTY IS EXPRESSED OR IMPLIED REGARDING THE ACCURACY OF THESE DATA OR THE RESULTS TO BE OBTAINED FROM THE USE THEREOF.

APPENDIX B

Data of Fall Cone Test

Test Number	1		2		3	
Cone penetration (mm)	14.50	14.40	17.90	17.75	23.40	23.10
Average penetration (mm)	14.45		17.83		23.25	
Container no.	11C/10	82C	29D	25C	43C	109C
Container weight (g)	9.79	9.96	10.34	9.93	10.83	10.54
Wet soil + container (g)	15.62	18.71	14.15	16.94	22.61	24.00
Wet soil, W_w (g)	5.83	8.75	3.81	7.01	11.78	13.46
Dry soil + container (g)	14.12	16.43	13.09	15.14	19.47	20.14
Dry soil, W_d (g)	4.33	6.47	2.75	5.21	8.64	9.60
Moisture loss, $W_w - W_d$ (g)	1.50	2.28	1.06	1.80	3.14	3.86
Moisture content (%)	34.64	35.24	38.55	34.55	36.34	40.21
Average moisture content (%)	34.94		36.55		38.28	

APPENDIX C

Data of Plastic Limit

Container no.	24C	90C/13a
Container weight (g)	10.42	10.00
Wet soil + container (g)	19.70	19.11
Wet soil, W_w (g)	9.28	9.11
Dry soil + container (g)	17.83	17.18
Dry soil, W_d (g)	7.41	7.18
Moisture loss, $W_w - W_d$ (g)	1.87	1.93
Moisture content (%)	25.24	26.88
Average moisture content (%)	26.06	

APPENDIX D

Data of Specific Gravity

Test No.	1	2	3	4	5
Density bottle no.	2/1B	2a/B2	3a/14	4/B1	4B/B4
Weight of density bottle (g)	31.71	32.59	31.88	33.15	31.90
Weight of bottle + Stopper (W_1) (g)	36.30	36.99	36.07	37.27	36.35
Weight of bottle + Stopper + Dry Soil (W_2) (g)	41.31	41.97	41.74	42.28	41.31
Weight of bottle + Stopper + Soil + Water (W_3) (g)	139.20	139.94	138.82	140.72	138.86
Weight of bottle + Stopper + Water (W_4) (g)	136.08	136.85	135.29	137.60	135.77
Weight of Dry Soil ($W_2 - W_1$) (g)	5.01	4.98	5.67	5.01	4.96
Weight of Water ($W_4 - W_1$) (g)	99.78	99.86	99.22	100.33	99.42
Weight of Water Used ($W_3 - W_2$) (g)	97.89	97.97	97.08	98.44	97.55
Specific gravity	2.65	2.63	2.65	2.65	2.65
Average Specific Gravity			2.65		

$$Specific\ Gravity, G_s = \frac{(W_2 - W_1)}{(W_4 - W_1) - (W_3 - W_2)}$$

APPENDIX E

Calculations in Determining Percent Passing of Soil Sample

$$Percent\ passing = \frac{\sum M - Cumulative\ Mass\ Retained}{\sum M} \times 100\ \%$$

Taking reading of 2.36 mm,

$$Percent\ retained = \frac{192.420 - 0.100}{192.420} \times 100\ \%$$
$$= 99.948\ \%$$

$$Percent\ retained = 100\ \% - Percent\ passing$$

Taking reading of 2.36 mm,

$$Percent\ retained = 100\ \% - 99.948\ \%$$
$$= 0.052\ \%$$

APPENDIX F

Basic Measurement and Calculations in Hydrometer Analysis

Basic measurement in hydrometer analysis:

Meniscus correction, cm	= -0.0005
Reading in dispersant, Ro	= 0.9985
Dry mass of soil, m	= 50 g
Particle density (measured/assume), ρ_s	= 2.65 Mg/m^3
Length of the bulb, h	= 164 mm
N	= 10 mm
Distance between the 100mL and the 1000mL, L	= 317 mm
Volume of hydrometer bulb, V_h	= 78.83 mL

Calculations:

True hydrometer reading,

$$R_h \ = \ R'_h + \ C_m$$

where:

C_m = meniscus correction

R'_h = observed hydrometer reading

Taking reading of 0.5 minute,

$$R_h = 1.0150 - 0.0005$$
$$R_h = 1.0145$$

APPENDIX F (Continued)

To calculate the H_R (in mm), corresponding to each of the major calibration marks, R_h from the following equation:

$$H_R = H + \frac{1}{2}\left[h - \frac{V_h L}{900}\right]$$

where:

H = length from the neck of bulb to graduation R_h

h = length of the bulb

V_h = volume of the hydrometer bulb

L = distance between the 100ml and 1000ml scale marking of the sedimentation cylinder.
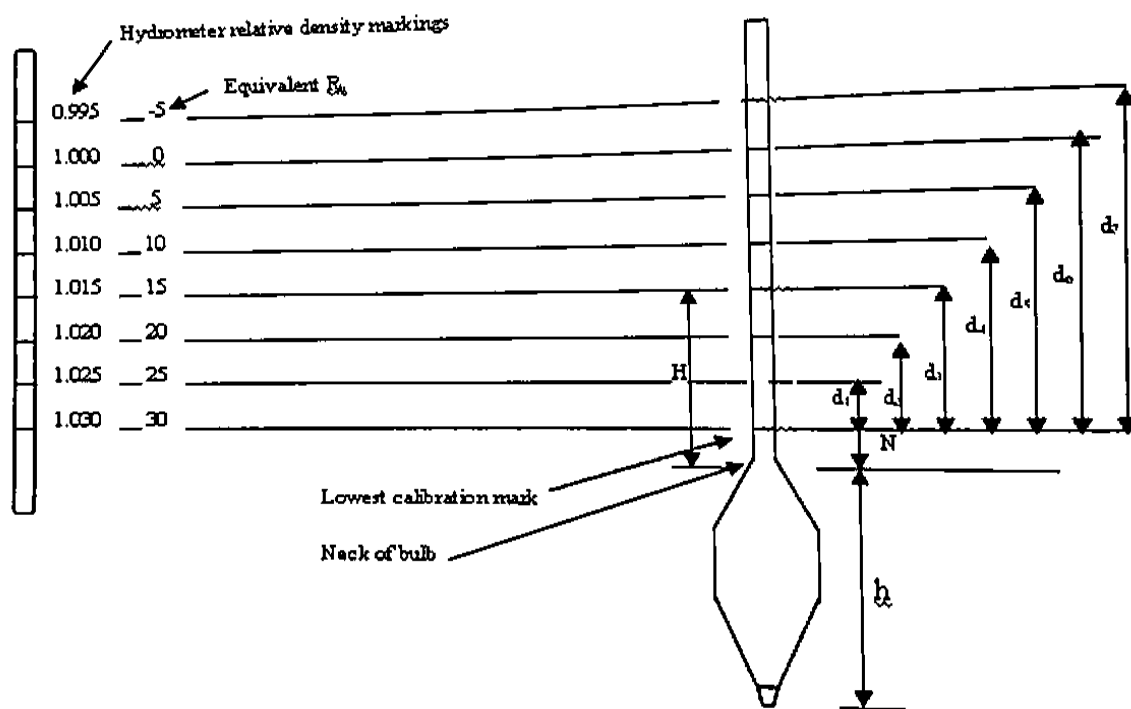
Figure F1: Essential measurements for calibration of hydrometer

APPENDIX F (Continued)

$H_n = N + d_n$

Example:

$$H_1 = N + d_1$$
$$= 10 + 19$$
$$= 29$$

$$H_R = 29 + \frac{1}{2}\left[164 - \frac{78.83 \times 317}{900}\right]$$
$$= 97.117161$$

Table F1: Data for plotting H_R versus R_h

N	d_n (mm)	H_n (mm)	R_h (mm)	H_R (mm)
1	19	29	1.025	97.11716
2	39	49	1.020	117.1172
3	59	69	1.015	137.1172
4	79	89	1.010	157.1172
5	99	109	1.005	177.1172
6	119	129	1.000	197.1172
7	140	150	0.995	218.1172
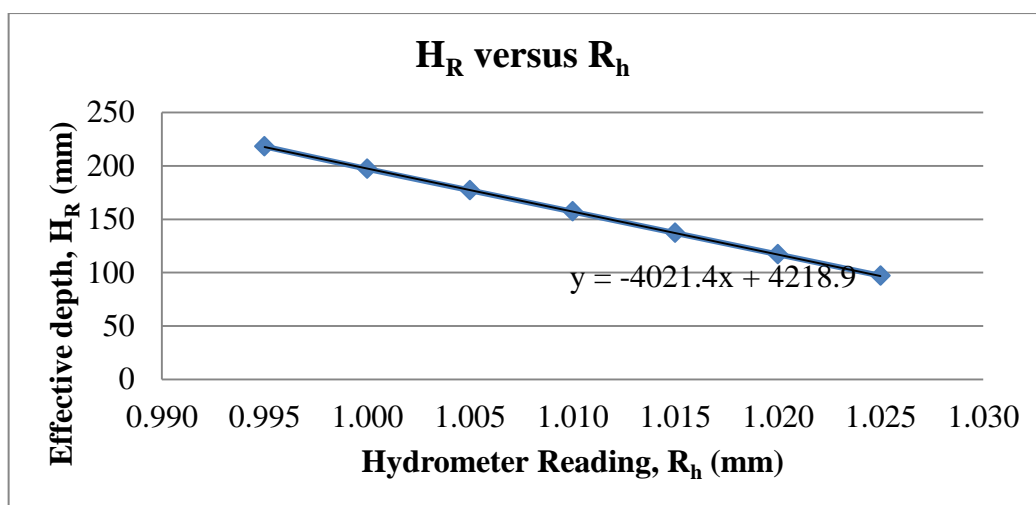
Figure F2: Graph of H_R versus R_h

APPENDIX F (Continued)

To obtain the effective depth, H_R by using equation obtained from the graph displayed in Figure 2:

$$y = -4021.4x + 4218.9$$

where:

x represents $R_h' + C_m$

Taking reading of 0.5 minute,

$$y = -4021.4(1.0145) + 4218.9$$
$$y = 139.1897$$

Equivalent particle diameter, D (mm):

$$D = 0.005531 \sqrt{\frac{\eta H}{(\rho_s - 1)t}}$$

where:

η = dynamic viscosity of water at test temperature as shown in Table 2

H = effective depth at which density of the suspension is measured (in mm)

ρ_s = particle density (in Mg/m^3)

T = elapsed time (in min)

Due to viscosity of water at 25.5 °C not given in Table 2, the intermediate value is obtained by using interpolation,

$$\eta = 0.8817$$

APPENDIX F (Continued)

Table F2: Viscosity of Water

Temperature T (˚C)	Viscosity of water, ŋ (mPa.s)
10	1.304
15	1.137
20	1.002
25	0.891
30	0.798

Taking reading of 0.5 minute,

$$D = 0.005531 \sqrt{\frac{(0.8871)(139.1897)}{(2.65 - 1)(0.5)}}$$

$$= 0.0675$$

Modified hydrometer reading,

$$R_d = R'_h - R'_o$$

where:

R'_o = hydrometer reading at the upper rim of the meniscus in the dispersion solution

Taking reading of 0.5 minute,

$$R_d = 1.015 - 0.9985$$

$$= 0.0165$$

APPENDIX F (Continued)

Percentage by mass of particles smaller than the corresponding equivalent diameter, D (in mm):

$$K = \left[\frac{100\rho_s}{m(\rho_s - 1)}\right] R_d$$

where:

m = mass of dry soil used (in g)

Taking reading of 0.5 minute,

$$K = \left[\frac{100(2.65)}{50(2.65 - 1)}\right] (0.0165)$$

$$K = 0.0530$$

APPENDIX G

Data of Falling Head Test

Measurements:

Diameter, Φ = 0.1007 m

Length, L = 0.131 m

Area, A = 0.00796 m^2
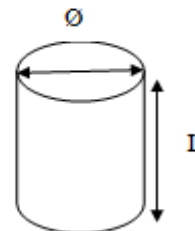
Manometer tube	T$_1$	T$_2$	T$_3$
Diameter (m)	0.01617	0.00733	0.00815
Start level, h$_1$ (m)	1.00000	1.00000	1.00000
End level, h$_2$ (m)	0.89400	0.56300	0.49400
h$_1$/h$_2$	1.11857	1.77620	2.02429
Log (h$_1$/h$_2$)	0.04866	0.24949	0.30627
Time, t (s)	900.00	900.00	900.00
Radius of manometer tube, r (m)	0.00809	0.00367	0.00408
Area of manometer, a (m^2)	0.00021	0.00004	0.00005
Area of permeameter, A (m^2)	0.00796	0.00796	0.00796
A x t (m^{2}s)	7.16400	7.16400	7.16400
Permeability coefficient, K$_t$ (m/s)	7.01699×10^{-12}	7.39266×10^{-12}	1.12192×10^{-11}
Average permeability coefficient (m/s)		8.54294×10^{-12}	

$$K_t = \frac{3.84 \times a \times L \times \log(\frac{h_1}{h_2}) \times 0.00001}{A \times t}$$

APPENDIX H

Typical Permeability Coefficient for Different Soils

Soil Type	Typical Permeability, k (cm/sec)
Gravels and Coarse Sand	$> 10^{-1}$
Fine Sand	10^{-1} to 10^{-3}
Silty Sand	10^{-3} to 10^{-5}
Silts	10^{-5} to 10^{-7}
Clay	$< 10^{-7}$

APPENDIX I

mi micromeritics

Full Report Set

MicroActive 4.00

ASAP 2020 V3.04
Serial # 1255 Unit 1

Page 1 of 65

Sample: KA
Operator: BEN
Submitter: UMP
File: C:\2020\data\001-501EDIT.SMP

Started: 4/4/2016 12:31:38 PM
Completed: 4/4/2016 4:11:11 PM
Report time: 4/11/2016 5:01:19 PM
Sample mass: 1.4011 g
Cold free space: 80.2677 cm³
Low pressure dose: None
Automatic degas: Yes

Analysis adsorptive: N2
Analysis bath temp.: -195.803 °C
Thermal correction: No
Warm free space: 16.0000 cm³ Entered
Equilibration interval: 5 s
Sample density: 1.000 g/cm³

Summary Report

Surface Area

Single point surface area at P/Po = 0.300407567: 1.8626 m²/g

BET Surface Area: 2.0160 m²/g

Langmuir Surface Area: 2.9333 m²/g

t-Plot Micropore Area: 0.5318 m²/g

t-Plot external surface area: 1.4842 m²/g

BJH Adsorption cumulative surface area of pores
between 17.000 Å and 3,000.000 Å width: 1.378 m²/g

BJH Desorption cumulative surface area of pores
between 17.000 Å and 3,000.000 Å width: 1.8714 m²/g

Pore Volume

Single point adsorption total pore volume of pores
less than 1,425.568 Å width at P/Po = 0.986236450: 0.007173 cm³/g

Single point desorption total pore volume of pores
less than 1,123.848 Å width at P/Po = 0.982465971: 0.008393 cm³/g

t-Plot micropore volume: 0.000216 cm³/g

BJH Adsorption cumulative volume of pores
between 17.000 Å and 3,000.000 Å width: 0.009647 cm³/g

BJH Desorption cumulative volume of pores
between 17.000 Å and 3,000.000 Å width: 0.009905 cm³/g

APPENDIX I (Continued)

mi micromeritics®

Full Report Set

Sample: KA
Operator: BEN
Submitter: UMP
File: C:\2020\data\001-501EDIT.SMP

Started: 4/4/2016 12:31:38 PM   Analysis adsorptive: N2
Completed: 4/4/2016 4:11:11 PM   Analysis bath temp.: -195.803 °C
Report time: 4/11/2016 5:01:19 PM   Thermal correction: No
Sample mass: 1.4011 g   Warm free space: 16.0000 cm³ Entered
Cold free space: 80.2677 cm³   Equilibration interval: 5 s
Low pressure dose: None   Sample density: 1.000 g/cm³
Automatic degas: Yes

Pore Size

Adsorption average pore diameter (4V/A by BET): 142.3144 Å

Desorption average pore diameter (4V/A by BET): 166.5253 Å

BJH Adsorption average pore width (4V/A): 279.953 Å

BJH Desorption average pore width (4V/A): 211.713 Å

APPENDIX J

LNAPL Migration in Aggregated Kaolin of 27 % Moisture Content

Image	Time (s)	Area (cm^2)	Percent area (%)	Mean Intensity (lum)	Saturation (lum)
1	5	5.057001487	0.050290033	66.72412851	50.31037383
2	10	6.998485175	0.069028223	64.93185156	46.54492419
3	15	8.149765863	0.079489772	65.80407045	46.70035225
4	20	8.707650031	0.085013599	73.77130623	52.02479944
5	25	8.864053235	0.087160893	78.88454003	56.27385808
6	30	9.016416112	0.089023659	80.04921719	56.02492895
7	35	9.957280797	0.097115569	76.67242214	54.28849973
8	40	10.23223572	0.100205021	78.01210219	54.95842512
9	45	10.81701996	0.105080177	76.4398443	53.96305143
10	50	10.99288053	0.107769314	76.31923784	53.66548989
11	55	11.41009751	0.110384113	75.18430649	53.33005945
12	60	11.87494782	0.116775057	75.52390631	53.28624895
13	70	12.20083213	0.118755433	75.21597488	53.06583821
14	80	12.70534144	0.124296583	76.18835219	53.3842388
15	90	13.24865917	0.12895434	75.98138131	52.87824824
16	100	13.95635443	0.135020984	74.56576161	51.70822477
17	110	14.09032318	0.136871785	81.95324298	51.33313714
18	120	14.3208345	0.14010885	81.3607172	53.05441384
19	135	14.85947395	0.14317678	78.06772995	52.38061335
20	150	15.60906102	0.152717702	76.70828849	54.10722995
21	165	15.9491928	0.154307875	75.72488695	52.95014166
22	180	16.38682407	0.15821562	76.9060565	54.24043446
23	200	16.67049759	0.164936882	79.91079094	55.41419998
24	220	18.35467621	0.180678214	80.3908285	54.86928616
25	240	19.40983963	0.190858394	79.88904409	54.23563568
26	270	19.79186323	0.191865709	76.16174222	55.29836258
27	300	21.32133983	0.208813374	76.38905207	54.44215608
28	360	21.43553225	0.208216498	77.08117854	55.64494928
29	420	21.53398865	0.208763854	78.25345585	56.33336625
30	480	23.38541556	0.228313991	78.78284624	56.74277543
31	540	25.55826116	0.249538046	79.11865934	56.55260421

APPENDIX J (Continued)

Image	Time (s)	Area (cm^2)	Percent area (%)	Mean Intensity (lum)	Saturation (lum)
31	540	25.55826116	0.249538046	79.11865934	56.55260421
32	600	27.31644157	0.270264641	85.12347226	56.12762537
33	720	31.74772392	0.310317735	79.14726177	57.46286417
34	840	34.62635094	0.333966057	78.71416918	58.13082996
35	960	38.02734977	0.36978976	77.5874989	58.07132312
36	1080	40.69109516	0.396875865	73.75267241	55.10953811
37	1200	42.67670348	0.416242265	68.41800579	50.68752709
38	1500	47.23440555	0.458813019	77.66360531	60.32260809
39	1800	52.40315399	0.513708311	78.4579425	62.92161076
40	2100	56.83879564	0.552670103	69.30152138	56.51511002
41	2400	61.06051257	0.591334352	60.62623958	49.21577092
42	3000	67.9158851	0.661046189	57.11292226	47.62395325
43	3600	75.73487573	0.731262364	62.50046142	58.33394637
44	4200	82.15112844	0.797183302	59.44433889	57.57757498
45	5400	93.83054568	0.911485532	52.97025812	55.66345909
46	5700	97.73924356	0.954241303	51.03431656	54.64407482

APPENDIX K

LNAPL Migration in Aggregated Kaolin of 29 % Moisture Content

Image	Time (s)	Area (cm^2)	Percent area (%)	Mean Intensity (lum)	Saturation (lum)
1	5	3.36229675	0.032461513	46.3898323	32.67071435
2	10	3.951014997	0.03787902	48.82325978	33.98920883
3	15	4.194497891	0.040170457	53.20324461	36.23470215
4	20	4.354728773	0.040834904	60.51268403	41.82037259
5	25	4.381947822	0.04179614	61.21458439	41.07085143
6	30	4.723355495	0.045281634	62.36068341	41.20840086
7	35	4.821067626	0.04598495	60.98639996	40.80528417
8	40	5.351094799	0.050989022	60.84824882	39.87176125
9	45	5.359281779	0.05116968	59.89385312	43.37954568
10	50	5.5305704	0.053288093	59.73591459	42.94511304
11	55	5.72812115	0.055134936	59.84434669	43.02968037
12	60	6.020087974	0.056796524	59.49862239	42.34473684
13	70	5.891010143	0.056306911	61.31479743	39.54822582
14	80	6.149697427	0.059195161	61.80362155	39.3499196
15	90	7.002100205	0.066924925	63.46714043	39.42190537
16	100	7.606660788	0.073592887	60.96405375	38.6158061
17	110	7.96274123	0.076105027	62.50445314	39.60772322
18	120	8.347741911	0.078600976	57.99146627	42.12671948
19	135	17.78435208	0.171527457	62.26518598	41.12468837
20	150	19.22483516	0.185440482	63.2211327	40.7339793
21	165	19.87692275	0.190748767	63.22766111	41.03098221
22	180	21.9075063	0.207082311	62.77160704	40.99817515
23	200	22.99456704	0.216310397	62.6439464	40.99311502
24	220	25.56176987	0.244803552	62.93525031	40.7432668
25	240	25.59430514	0.243633835	61.55206139	40.78540539
26	270	27.40373391	0.258773387	62.51386879	41.03797282
27	300	28.54470113	0.270925292	61.84949044	40.54367746
28	360	29.62687096	0.281456057	63.01266601	40.63771237
29	420	31.36410546	0.30345254	62.28173523	40.87058664
30	480	34.3377865	0.330515187	61.64386046	40.12389109
31	540	36.43365322	0.35069163	60.97990846	40.10613865
32	600	38.57970507	0.371341582	61.03938369	40.22033683

APPENDIX K (Continued)

Image	Time (s)	Area (cm^2)	Percent area (%)	Mean Intensity (lum)	Saturation (lum)
33	720	41.77762429	0.396089967	60.03496926	40.01810519
34	840	44.80946478	0.433936639	58.70923886	40.67902031
35	960	49.23224117	0.46866811	57.62421011	40.40230823
36	1080	55.28571501	0.524705897	56.81707605	40.09228766
37	1200	58.99441668	0.567266493	54.8553659	39.06568767
38	1500	68.35192149	0.655915372	54.46697995	40.70257847
39	1800	78.32557625	0.741142501	52.85040348	40.96379363
40	2100	86.93625842	0.825890079	51.91539544	41.03648623
41	2400	94.93419303	0.906424039	50.65342365	41.23187956
42	2520	98.8323648	0.939971564	50.56056714	41.51550989

APPENDIX L

LNAPL Migration in Aggregated Kaolin of 31 % Moisture Content

Image	Time (s)	Area (cm^2)	Percent area (%)	Mean Intensity (lum)	Saturation (lum)
1	5	20.73751251	0.191251124	28.66567884	26.86870898
2	10	28.16852538	0.260772504	30.632016	27.92256068
3	15	35.93531072	0.334006001	33.18230279	30.82563954
4	20	42.80014612	0.395165265	35.7710845	32.14974301
5	25	45.029131	0.419373653	34.21667883	32.12727298
6	30	50.24838354	0.465777875	35.0658365	32.42099049
7	35	56.28186839	0.517025454	35.71581016	32.71017926
8	40	59.0367338	0.55809954	35.24214274	32.63123885
9	45	67.15045568	0.62413973	36.54152878	32.76845029
10	50	67.25826863	0.635177688	35.53293886	32.89024876
11	55	74.79932726	0.695288942	36.78834287	33.24985892
12	60	78.45667424	0.730022062	37.06533189	33.10584104
13	70	84.67473827	0.7863146	36.87997663	33.52242708
14	80	87.03258833	0.812228924	36.7899063	33.59441065

APPENDIX M

LNAPL Migration in Aggregated Kaolin of 33 % Moisture Content

Image	Time (s)	Area (cm^2)	Percent area (%)	Mean Intensity (lum)	Saturation (lum)
1	5	15.13410989	0.138711284	57.3651494	46.32201997
2	10	15.99799571	0.147212805	62.28174846	46.67171549
3	15	18.67513797	0.171675242	59.93380702	46.7421645
4	20	19.49979008	0.177319083	60.10257235	46.49649671
5	25	19.6802226	0.177737661	58.44042191	46.10619354
6	30	22.04253829	0.201430615	59.22013628	45.49859151
7	35	23.72671691	0.215121368	61.26251229	46.19267412
8	40	25.57793118	0.22921256	59.71319463	45.3255378
9	45	25.49095781	0.231121098	62.14194686	47.3805887
10	50	26.01045887	0.231953274	61.59562692	47.67712042
11	55	28.00329725	0.251666222	63.66224586	48.89986559
12	60	29.10726357	0.263129616	64.03999381	48.75257069
13	70	33.33876236	0.302271395	65.54992978	49.11713341
14	80	34.44995875	0.309603688	63.95936829	48.59821671
15	90	34.67813093	0.313800309	64.13269703	49.33163782
16	100	35.57763542	0.320990828	63.75353492	49.72135057
17	110	39.21393016	0.356587334	63.61971346	49.17606436
18	120	42.60844321	0.375913189	64.30735223	49.70795279
19	135	47.15923419	0.42883828	61.16512867	44.4638782
20	150	47.86746107	0.433573586	59.27398368	43.43582881
21	165	51.29121333	0.464126622	60.08881993	43.73095524
22	180	52.19039885	0.462682628	57.96715085	42.69211384
23	200	54.25681371	0.48429697	59.08687655	43.60001568
24	220	59.36506357	0.535084239	60.52181858	45.87209384
25	240	61.8286001	0.556747648	61.16053463	46.31857632
26	270	63.41134523	0.576063418	58.54626939	44.84390044
27	300	69.65428917	0.637782451	52.07265537	38.43027517
28	360	77.84860496	0.703754646	53.50335664	37.41490207
29	420	85.93287498	0.778362251	53.4584351	37.22133989
30	480	91.76593832	0.827170823	55.30014811	39.30367697